



UNIVERSITÀ DI PARMA

UNIVERSITÀ DEGLI STUDI DI PARMA

DOTTORATO DI RICERCA IN SCIENZE MEDICO VETERINARIE

CICLO XXXVII

Feline Nasal Planum Squamous Cell Carcinoma: interaction between Feline Papillomavirus infection and Epithelial–Mesenchymal Transition

Coordinatore:

Chiar.mo Prof. Donofrio Gaetano

Tutor:

Chiar.ma Prof.ssa Di Lecce Rosanna

Dottorando: Dott.ssa Guarnieri Chiara

Anni Accademici 2021/2022 – 2024/2025

Contents

ABSTRACT	3
RIASSUNTO	4
1 – INTRODUCTION	6
2 – FELINE NASAL PLANUM SQUAMOUS CELL CARCINOMA	8
2.1 FELINE SQUAMOUS CELL CARCINOMA	8
2.1.1. Histopathological features.....	8
2.1.2 Incidence and prevalence.....	8
2.1.3 Predisposing factors	8
2.1.4 Anatomical sites	9
2.2 NASAL PLANUM SQUAMOUS CELL CARCINOMA	9
2.2.1 Epidemiology and predisposing factors.....	9
2.2.2 Pathogenesis	10
2.2.3. Clinical, cytological and histopathological features	10
2.2.4 Treatments and prognosis	11
2.3 UV-INDUCED PRE-NEOPLASTIC LESIONS OF THE FELINE NASAL PLANUM.....	12
3 – FELIS CATUS PAPILOMAVIRUS	13
3.1 GENERAL VIROLOGY OF PAPILOMAVIRUSES IN DOMESTIC CARNIVORES	13
3.2 CLASSIFICATION AND MOLECULAR TYPING OF FCAPV	14
3.3 VIRAL ONCOGENESIS.....	15
3.3.1 Role of E6/E7 proteins in cell cycle deregulation.....	16
3.3.2 Molecular mechanisms of virus-host interaction	17
3.4 EXPERIMENTAL AND CLINICAL EVIDENCE OF THE FCAPV-SCC ASSOCIATION.....	18
4 – EPITHELIAL-MESENCHYMAL TRANSITION	20
4.1 DEFINITION AND BIOLOGICAL RELEVANCE OF EMT	20
4.2 EMT IN EMBRYONIC LIFE	21
4.3 EMT IN WOUND HEALING, TISSUE FIBROSIS AND INFLAMMATION	22
4.3.1 EMT in wound healing	23
4.3.2 EMT in fibrosis	23
4.3.3 EMT and inflammation	24
4.4 EMT IN EPITHELIAL TUMORS.....	25
4.4.1 Molecular mechanisms	25
4.4.2 Role in tumor progression, invasion and metastasis	26

4.4.3 EMT and therapeutic resistance	27
4.5 EMT MOLECULAR MARKERS	29
4.5.1 Epithelial markers	29
4.5.2 Mesenchymal markers	30
4.5.3 Transcription factors	32
5 – INTERPLAY BETWEEN PVS AND EMT	34
5.1 VIRAL ONCOPROTEINS AS INDUCERS OF EMT	34
5.2 EVIDENCE FROM HUMAN MEDICINE: HPV-INDUCED EMT IN HNSCC	35
5.3 FCAPV AND EMT: SYNERGISTIC ROLE IN TUMOR PROGRESSION	36
5.4 COMPARATIVE ONCOLOGY: INSIGHTS FROM CANINE, EQUINE AND HUMAN SCC MODEL	38
6 – RESEARCH AIMS AND OBJECTIVES	41
7 – MATERIALS AND METHODS.....	42
7.1 CASE SELECTION	42
7.2 HISTOLOGICAL EVALUATIONS	42
7.3 IMMUNOHISTOCHEMISTRY	42
7.4 DNA EXTRACTION AND FCAPV DETECTION	44
7.5 RNA EXTRACTION, cDNA SYNTHESIS AND VIRAL ONCOGENE EXPRESSION ANALYSIS	47
8 – RESULTS	51
8.1 IMMUNOHISTOCHEMICAL EVIDENCE OF EMT.....	51
8.2 FCAPV MOLECULAR DETECTION.....	55
8.3 EVALUATION OF ONCOGENE EXPRESSION	57
8.4 CORRELATION BETWEEN FCAPV STATUS AND IMMUNOHISTOCHEMICAL FINDINGS.....	57
9 – DISCUSSION	61
10 – CONCLUSION	67
BIBLIOGRAFIA	68

Abstract

Feline nasal planum squamous cell carcinoma (npSCC) is a locally aggressive neoplasm of great relevance in veterinary oncology. Beyond its clinical relevance in cats, npSCC has attracted growing interest as a potential comparative model for human papillomavirus (HPV)-associated carcinomas, for its histopathological and molecular similarities. In particular, the detection of viral DNA and transcriptional activity of viral oncogenes in feline SCC suggests a biologically active role rather than incidental infection. At the same time, epithelial-mesenchymal transition (EMT) has been recognized as an important process in the progression and invasiveness of squamous cell carcinomas across species. However, the interplay between FcaPV infection and EMT activation in feline npSCC remains incompletely defined, representing an important topic of study with both clinical and comparative oncology implications.

The aim of the study was to investigate the prevalence and transcriptional activity of FcaPV in feline npSCC, the expression of EMT markers and to explore associations between viral infection status and EMT features. Fifty feline npSCC and ten control tissues were examined by PCR and RT-PCR for FcaPV DNA and E6/E7 transcription, and by immunohistochemistry for epithelial, mesenchymal, EMT transcription factors and hypoxia/ β -catenin pathway markers.

FcaPV DNA was detected in 64% of npSCC, predominantly FcaPV-2. Viral transcription was confirmed in 95% of L1-positive tumors, supporting biologically active infection. Immunohistochemistry revealed EMT features, including loss of epithelial markers, vimentin acquisition and focal nuclear expression of TWIST-1 and ZEB1. However, no significant differences in EMT markers expression were found between FcaPV-positive and FcaPV-negative tumors.

These findings confirm that FcaPV is actively involved in feline npSCC, but EMT activation appears as a common feature of SCC progression independent of viral status. Further studies are needed to continue to evaluate feline npSCC as a model for studying PV-induced tumorigenesis in perspective.

Riassunto

Il carcinoma squamocellulare del planum nasale del gatto (npSCC) è una neoplasia localmente aggressiva, di rilevante interesse clinico in medicina veterinaria. Negli ultimi anni l'attenzione nei confronti di questa patologia è cresciuta anche per il suo potenziale valore come modello spontaneo di studio dei carcinomi squamocellulare associati all'infezione da papillomavirus nell'uomo. In particolare, la dimostrazione della presenza del DNA virale e dell'attività trascrizionale degli oncogeni virali nei tumori felini suggerisce un ruolo biologicamente attivo dell'infezione da papillomavirus felino, piuttosto che una semplice presenza accidentale del virus nel tessuto neoplastico. Parallelamente, l'epithelial-mesenchymal transition (EMT) è ampiamente riconosciuto come un processo chiave nella progressione, nell'invasività e nel potenziale metastatico dei carcinomi squamocellulari in diverse specie. Tuttavia, l'interazione tra infezione da FcaPV e attivazione dell'EMT nell'npSCC felino rimane ancora poco chiara, rappresentando un ambito di ricerca di grande interesse, che potrebbe avere conseguenze sia nel contesto dell'oncologia comparata sia nel concetto di One Health.

Lo scopo di questo studio è stato quello di indagare la prevalenza dell'infezione da FcaPV e la sua attività trascrizionale nei npSCC felini, valutare l'espressione dei marcatori immunostochimici di EMT e analizzare l'eventuale associazione tra stato di infezione virale e caratteristiche di EMT. A tal fine, sono stati esaminati 50 campioni di npSCC e 10 campioni di controllo, mediante PCR e RT-PCR per la ricerca del DNA virale e dell'espressione degli oncogeni E6/E7, e mediante immunostochimica per i marker epiteliali, mesenchimali, l'HIF-1 α , la β -catenina e i fattori di trascrizione EMT-correlati TWIST-1 e ZEB1.

Il DNA di FcaPV è stato rilevato nel 64% dei tumori analizzati e l'espressione degli oncogeni virali è stata confermata nel 95% dei tumori L1-positivi, indicando la presenza di una infezione biologicamente attiva. L'analisi immunostochimica ha mostrato caratteristiche compatibili con l'attivazione dell'EMT, tra cui la riduzione dei marker epiteliali, l'aumento della positività alla vimentina e l'espressione nucleare focale di TWIST-1 e ZEB1. Tuttavia, il confronto tra tumori FcaPV-positivi e FcaPV-negativi non ha evidenziato differenze statisticamente significative nei pattern di espressione dei marcatori di EMT.

Nel complesso, i risultati dello studio supportano il coinvolgimento attivo del FcaPV nella patogenesi del npSCC felino, ma suggeriscono che l'attivazione dell'EMT rappresenti un evento comune nella progressione del carcinoma squamocellulare, indipendentemente dallo stato dell'infezione virale. Sono necessari ulteriori studi per approfondire il ruolo prognostico e biologico dell'interazione tra infezione da papillomavirus ed EMT, e per consolidare il carcinoma squamocellulare del planum nasale felino come modello di studio dei tumori papillomavirus-indotti in una prospettiva di oncologia comparata e One Health.

1 – INTRODUCTION

Squamous cell carcinoma (SCC) is a malignant neoplasm of epidermal origin, in which tumor cells exhibit varying degrees of keratinocytes differentiation (1,2). SCC represents approximately the 15% of feline skin tumors and the majority of feline oral malignant tumor (2–4). It is considered one of the most frequent skin tumors in cats, especially in areas with limited pigmentation and poor hair coverage such as nasal planum, eyelids and auricular pinnae (1,2). Clinically, feline cutaneous SCC, frequently presents as insidious ulcerative or crusting lesions, which are often indistinguishable from chronic inflammatory or actinic dermatoses, complicating differential diagnosis and potentially delaying treatment (2,5,6).

SCC typically exhibits locally invasive growth with a relatively low metastatic rate (< 10%), although more aggressive behaviour has been observed in poorly differentiated or mucosal forms (2,7). Treatment options include surgical excision, cryotherapy, photodynamic therapy (PDT) and radiotherapy, with variable outcomes depending on tumor size, depth of invasion and anatomical site (6,8,9). Prognosis is generally favourable when the lesion is early diagnosed and completely excised with adequate surgical margins (2,5,10).

Over the past decade, there has been growing interest in feline epithelial tumors, in particular squamous cell carcinoma, as a model for comparative oncology research. Feline cutaneous SCC shares multiple features with its human counterparts, like UV-induced pathogenesis, histopathological traits and a typically locally aggressive behaviour (2–4).

Recent studies have highlighted the role of *Felis catus* papillomavirus (FcaPV) as a potential cofactor in the pathogenesis of SCC, in particular in UV-protected areas, such as the oral cavity and perineum, where viral DNA and oncogene expression have been detected (3,11,12).

Furthermore, the investigation of epithelial-mesenchymal transition (EMT) in feline SCC, particularly at oral and nasal sites, has revealed crucial molecular events associated with aggressive tumor behaviour and resistance to conventional therapies (13,14). Studies in comparative oncology have shown that equine papillomavirus type 2 (EcPV2) can promote EMT in SCC of the larynx, penis and vulva by upregulating transcription factors like TWIST-1, ZEB1 and Snail, and by

activating the Wnt/ β -catenin signalling pathway (15,16). It would be of interest to determine whether FcaPV may similarly contribute to tumor progression by inducing EMT in feline SCC.

Understanding the interplay between viral infection and EMT in feline SCC could offer new insights into tumor biology and provide new diagnostic, prognostic and therapeutic strategies with relevance for both veterinary and human medicine.

This thesis aims to investigate the potential interaction between *Felis catus* papillomavirus (FcaPV) infection and the process of epithelial-mesenchymal transition (EMT) in squamous cell carcinoma (SCC) of the nasal planum in cats. Moreover, by drawing parallels with models in human (HPV-related) and equine (EcPV2-related) squamous cell carcinomas, this work contextualizes the feline disease within a broader comparative oncology framework, enhancing its translational relevance.

It is hypothesized that FcaPV infection, particularly genotype FcaPV-2, may act as an oncogenic promoter, triggering or facilitating the EMT process in feline nasal planum SCC.

Specific objectives include:

- To detect FcaPV DNA in nasal planum SCC samples by polymerase chain reaction (PCR)
- To evaluate the expression of EMT markers using immunohistochemistry
- To analyse correlations between FcaPV infection status and EMT features
- To compare findings with data from the human literature, particularly studies on HPV-associated head and neck squamous cell carcinoma.

2 – FELINE NASAL PLANUM SQUAMOUS CELL CARCINOMA

2.1 Feline squamous cell carcinoma

2.1.1. Histopathological features

Feline squamous cell carcinoma (SCC) is a malignant epithelial neoplasm characterized by the proliferation of atypical squamous epithelial cells with variable degrees of keratinization. Histologically, SCC are composed of infiltrative lobules or cords of neoplastic keratinocytes with marked cellular pleomorphism, prominent intercellular bridges and often keratin pearl formation. Areas of necrosis, stromal desmoplasia and inflammatory infiltration may also be present (1).

Tumor grading is based on the degree of cellular differentiation, mitotic index and keratin production. Well-differentiated SCC display distinct squamous morphology and abundant keratinization, whereas poorly differentiated variants may resemble anaplastic carcinomas and are associated with more aggressive biological behaviour (10,11,13).

2.1.2 Incidence and prevalence

SCC represents one of the most common skin tumors in cats, accounting approximately 15% of all feline skin tumors and constituting the most prevalent malignant oral tumor in this species (1,2). The disease primarily affects middle-aged and senior cats, with most cases diagnosed in animals older than 9 years. No consistent sex predilection has been observed (7). It is especially observed in outdoor-living and lightly pigmented cats (6).

2.1.3 Predisposing factors

Several predisposing factors contribute to the development of feline SCC, but the most significant is chronic UV radiation exposure. UV-induced DNA damage, particularly in the absence of melanin-mediated protection, promotes mutagenesis in key regulatory genes such as TP53, a tumor suppressor (2,3).

Other recognized risk factors are:

- Coat colour. White or lightly pigmented cats are over-represented among SCC cases in sun-exposed areas (2,3).
- Age. Older cats are at higher risk, possibly due to cumulative UV exposure and age-related decline in DNA repair efficiency (2,5).
- *Felis catus* papillomavirus (FcaPV) infection. In UV-protected anatomical regions, FcaPV, in particular genotypes 2 and 4, has been implicated as a co-carcinogenic agent (3,11,12,17).

2.1.4 Anatomical sites

Feline SCC arises in both cutaneous and muco-cutaneous sites, which can be broadly categorized based on their exposure to ultraviolet light: UV-exposed sites include the nasal planum, auricular pinnae, eyelids and periorbital skin; UV-protected sites include the oral cavity, perineal and anogenital regions, digits or subungual tissue (1,18).

Cutaneous SCC, particularly those of the nasal planum, often exhibit an indolent but locally aggressive course, and typically require wide surgical excision for a good management. In contrast, oral SCC are generally more aggressive, with early bone involvement and a poorer prognosis and limited treatment options (2,4,14).

Recent studies have also documented histopathological and molecular differences between SCC depending on the anatomical location and suspected etiology (UV-induced versus FcaPV-associated), supporting the need for anatomical site-specific diagnostic and therapeutic approaches (11,13,14).

2.2 Nasal planum squamous cell carcinoma

2.2.1 Epidemiology and predisposing factors

Nasal planum squamous cell carcinoma (npSCC) is one of the most common cutaneous tumors in cats. It predominantly affects geriatric cats, typically over nine years of age and it is strongly associated with chronic photodamage, especially in white or lightly pigmented cats (2,19).

Epidemiological data indicate that cats with outdoor access and prolonged sun exposure are at significantly increased risk for npSCC, with a clear anatomical predilection for non-pigmented, hairless areas such as the nasal planum (7). Seasonal fluctuations in incidence have also been reported, with peaks during the sunnier months (10,12).

FcaPV DNA has occasionally been detected in npSCC, but most cases are considered UV-induced. In contrast to papillomavirus-associated SCC, which typically arise in UV-protected regions, npSCC is usually classified as a photo-carcinoma, with UV radiation playing a central role in DNA damage and tumor progression (11,20).

2.2.2 Pathogenesis

The pathogenesis of npSCC is primarily driven by cumulative DNA damage from chronic UV exposure. UV-B radiation creates specific DNA lesions in keratinocytes, which can lead to mutations in important suppressor genes like TP53 (2,3).

Histopathological progression includes solar keratosis, epidermal dysplasia and eventual neoplastic transformation. This pathway mimics actinic carcinogenesis observed in human dermatopathology (10,21,22).

Although the role of FcaPV in npSCC remains controversial, its contribution seems to be secondary. In contrast to SCC of the oral cavity or perineal region, where expression of viral oncogenes such as E6 and E7 is consistently observed, npSCC lesions show low rates of viral DNA or transcriptional activity, reinforcing the predominance of UV-driven oncogenesis in this anatomic site (6,11).

2.2.3. Clinical, cytological and histopathological features

Clinically, npSCC typically presents as a slowly, progressive, ulcerative or crusted lesion on the nasal planum. This lesion may initially resemble chronic inflammation, actinic dermatitis or a non-healing wound (2). In more advanced cases, the tumor can cause deformation of the nasal architecture and, in some instances, extension into the nasal cavity or underlying bone (2).

Cytological examination (e.g. fine-needle aspiration or impression smears) often reveals pleomorphic squamous epithelial cells, keratin debris and a mixed inflammatory infiltrate, but for a certain diagnosis histopathology is needed (23).

Histologically, npSCC is characterized by:

- Infiltrative islands and cords of neoplastic keratinocytes
- Variable keratinization (from well-differentiated to poorly differentiated)
- Invasive growth into dermis and subcutaneous tissue
- Ulceration and secondary bacterial colonization are common (1,3).

Features of actinic damage, such as solar elastosis and epidermal dysplasia, are frequently observed in surrounding tissue. Immunohistochemical evaluation may show altered p53 expression, loss of E-cadherin and occasional positivity for vimentin, particularly in aggressive or recurrent tumors indicating EMT involvement (13).

2.2.4 Treatments and prognosis

Management of npSCC requires a multimodal strategy based to tumor size, invasiveness and owner preferences. The gold standard of treatment is surgical excision, ideally with 3-5 mm margins, although complete resection may be impactful from an aesthetic and functional point of view (2,12).

Adjunctive or alternative therapeutic modalities include:

- Cryotherapy. Indicated for superficial or early-stage lesions, however, recurrence rates are high with incomplete margins (12).
- Photodynamic therapy (PDT). Effective in selected early cases, requires multiple sessions and strict post-treatment photoprotection (24).
- Radiotherapy. Accelerated fractionation protocols (e.g. 10 x 4.8 Gy) have yielded > 90% complete remission and median survival times exceeding 900 days (5).
- Electrochemotherapy (ECT). Combines chemotherapy agents (e.g. bleomycin) with permeabilizing electric pulses. Recent studies describe a 100% objective response rate in npSCC, with median progression-free intervals of up 12 months (6,9).

Prognosis is closely linked to early detection and complete surgical excision. Although local recurrence is relatively common in incompletely treated or aggressive tumors, distant metastasis remains rare (< 10%) (1,12). With appropriate therapy, quality of life is generally preserved and cosmetic outcomes are often satisfactory (10,12).

2.3 UV-induced pre-neoplastic lesions of the feline nasal planum

Chronic ultraviolet (UV) radiation exposure is a primary etiological factor in the development of actinic keratosis and subsequent SCC of the nasal planum in cats. This condition predominantly affects lightly pigmented, outdoor cats due to sparse melanin protection (20,25).

UV radiation induces DNA lesions leading to mutations in key tumor suppressor genes such as TP53, and promotes oxidative stress, chronic inflammation and localized immunosuppression. These changes create a permissive microenvironment for carcinogenesis progressing through epidermal hyperplasia, dysplasia, carcinoma in situ and invasive SCC (25).

UV radiation induces a spectrum of histologically and clinically identifiable pre-neoplastic changes. These include:

- Actinic keratosis-like lesions, characterized by hyperkeratosis, epidermal hyperplasia and variable degrees of keratinocyte atypia with preserved basement membrane integrity.
- Solar elastosis, a hallmark of chronic photodamage, defined by basophilic degeneration of dermal collagen and elastin fibers due to UV-induced matrix metalloproteinase (MMP) activation (26,27).
- Atypical squamous hyperplasia, in which keratinocytes display nuclear pleomorphism, increased mitotic activity and loss of orderly maturation, features which may overlap with carcinoma in situ (28).

Early interventions targeting actinic keratosis and carcinoma in situ, such as curettage with diathermy, yield high complete remission rate (> 90%) in cats with superficial lesions (29). Alternative treatments like photodynamic therapy also show favourable initial response (85-96%), though recurrence is common (24).

3 – FELIS CATUS PAPILOMAVIRUS

3.1 General virology of papillomaviruses in domestic carnivores

Papillomaviruses (PV) are small, non-enveloped DNA viruses with a circular, double-stranded genome of approximately 8 kilobases. They exhibit a strong epithelial tropism, infecting basal keratinocytes through micro-abrasions and exploiting the host cell machinery during differentiation. PVs are known for their high species specificity and for establishing persistent infections, often asymptomatic, in the cutaneous and mucosal epithelia of a wide range of vertebrate hosts (3,30). In immunocompetent hosts, infections are typically asymptomatic and self-limiting, but persistent infections, particularly with oncogenic PV types, can lead to hyperplastic, dysplastic or neoplastic lesions (31).

The PV genome is divided into three functional regions: the early region (E), encoding proteins involved in replication and oncogenesis (E1, E2, E3, E4, E5, E6, E7), the late region (L), encoding the capsid proteins L1 and L2, and the upstream regulatory region (URR), which contains promoter and enhancer elements that regulate transcription and replication (32,33). Classification of PVs is based on sequence identity of the gene L1, the most conserved genomic region. There is a high level of viral diversity across hosts and new types continuing to be identified as sequencing technologies advance (32).

The PV life cycle is closely related to the differentiation of stratified squamous epithelial cells. After infecting basal keratinocytes, the virus establishes a persistent infection by maintaining its genome in an episomal state with low level replication. As the host cells undergo differentiation, the virus initiates its productive cycle, resulting in active viral replication and formation of new virions in the superficial layers of the epithelium. In oncogenic PV types, the expression of early genes, like E6 and E7, interferes with normal cell cycle regulation, promoting uncontrolled cell proliferation and genomic instability (3,34).

In domestic carnivores, PVs have been described in both dogs and cats. Canine papillomaviruses (CPV) include several genotypes, with CPV-1 being the most commonly reported and associated with oral papillomatosis in young dogs (31,35). Other CPV types, such as CPV-2 and CPV-16, have been identified in cutaneous and mucosal squamous cell carcinomas (36,37). Despite this, the

oncogenic role of CPV remains uncertain and studies have shown limited association between p16 expression and PV DNA in canine SCC (38,39).

In cats, *Felis catus* papillomaviruses (FcaPV) have gained increasing attention due to their more consistent association with neoplastic progression. FcaPV-2 is the most commonly implicated in cutaneous and oral SCC (40,41). These viruses are associated with a wide spectrum of lesions, from benign viral plaques and Bowenoid in situ carcinoma to invasive squamous cell carcinoma (11,18,42).

3.2 Classification and molecular typing of FcaPV

Felis catus papillomaviruses (FcaPV) represent a diverse group of papillomaviruses infecting domestic cats, classified into different genera based on the sequence of the L1 gene, which encodes the major capsid protein. Until recently, ten distinct feline papillomavirus types (FcaPV-1 to FcaPV-10) had been identified and classified (31,40,43).

- FcaPV-1, belonging to the genus *Lambdapapillomavirus*, was the first to be identified and is typically associated with oral papillomas and viral plaques. It's not been linked to malignant transformation (3,30).
- FcPV-2 is the most extensively studied type and belongs to the genus *Dyothetapapillomavirus*. It's been consistently detected in both benign and malignant lesions, including cutaneous SCC, oral SCC and Bowenoid in situ carcinoma (40). Its oncogenic potential is supported by evidence of E6/E7 transcriptional activity and p53 degradation in vitro and in vivo (44).
- FcaPV-3 to FcaPV-10 grouped within the genus *Taupapillomavirus*. FcaPV-3, FcaPV-4 and FcaPV-5 have been identified in cats with viral plaques, Bowenoid in situ carcinoma and, in some cases, invasive SCC. Although their pathogenic significance is less well defined than that of FcaPV-2, several studies have reported their presence in neoplastic lesions, raising the possibility of oncogenicity (17,42). While FcaPV-6 through FcaPV-10 have been more rarely identified, with their clinical significance still under investigation (45).

Most recently, FcaPV-11 has been identified and genetically characterized by Munday et al. (45), representing the first feline papillomavirus classified within the genus *Treisetapapillomavirus*.

Although its pathogenic role has not yet been established, the identification of FcaPV-11 brings the number of recognized feline papillomavirus types to eleven, reinforcing the idea that feline PV diversity remains underestimated.

Due to the increasing number of PV discovered in feline skin and mucosa, molecular typing has become essential to distinguish between them and to identify which ones may play a role in tumor development. The most used method is polymerase chain reaction (PCR), which targets conserved regions of the viral genome, such as the L1 or E1 genes. After amplification, the PCR products are sequenced to determine the specific viral type. If the virus is novel or genetically divergent a more advanced techniques like rolling circle amplification (RCA) or next-generation sequencing (NGS) can be used to recover the complete viral genome (42,46).

However, simply detecting viral DNA in a lesion is not enough to prove that the virus is causing the tumor. To demonstrate a causal role in oncogenesis, researchers have used additional molecular techniques to confirm active viral gene expression. These include: in situ hybridization (ISH), which shows where viral RNA is located in the tissue; reverse transcription PCR (RT-PCR), which detects RNA transcripts of viral oncogenes; RNAscope, a highly sensitive RNA-based technique that localizes viral mRNA, particularly E6 and E7, within tumor cells (11,34).

Another important marker is p16(INK4a) overexpression, which is often used in human medicine as an indirect indicator of papillomavirus activity. Similar to HPV-related tumor in humans, increased expression of p16 has been observed in FcaPV-associated feline lesions, further suggesting a functional role for the virus in tumor development (14,19).

3.3 Viral oncogenesis

Papillomaviruses are known for their capacity to induce epithelial neoplasia through the expression of viral oncogenes (30). The viral protein E6 and E7 interact with key host regulatory pathways, leading to loss of cell control, genomic instability and apoptosis evasion, which collectively promote tumorigenesis (34,44,47). Among *Felis catus* papillomaviruses, FcaPV-2 has demonstrated the strongest oncogenic potential and has been repeatedly implicated in feline cutaneous and oral SCC (40,48).

Moreover, transcriptional expression of E6 and E7 has been demonstrated in FcaPV-associated feline SCC tissues, confirming the biological activity of these viral genes within the tumor microenvironment (40,47). These molecular features highlight a critical role for viral oncogenes not only in tumor initiation, but also potentially in tumor progression, including through activation of EMT pathways (49).

3.3.1 Role of E6/E7 proteins in cell cycle deregulation

The oncogenic activity of PV is primarily driven by two early viral proteins: E6 and E7. These proteins are encoded by the viral genome and expressed early during infection. In oncogenic papillomaviruses they interfere with key tumor suppressor pathways, leading to loss of cell cycle control, genomic instability and ultimately, neoplastic transformation (11,43).

The E6 protein binds to the cellular protein p53. Under normal conditions p53 regulates the cell cycle, initiates apoptosis in response to DNA damage and maintains genomic stability. In papillomavirus-infected cells, E6 forms a complex with E6-associated protein and promotes proteasomal degradation of p53 via the ubiquitin-proteasome pathway. This degradation of p53 removes a critical checkpoint in the cell's defence against transformation, promoting clonal expansion of abnormal cells (44,47).

The E7 protein targets another key tumor suppressor: the retinoblastoma protein (pRb). Under normal physiological conditions, pRb binds and inhibits E2F transcription factors, preventing inappropriate entry into the S phase of the cell cycle. E7 binds directly to pRb, leading to its functional inactivation or degradation (11,32). This uncontrolled cell cycle progression, combined with the inhibition of apoptosis, creates a cellular environment favourable to neoplastic transformation (50,51).

Together E6 and E7:

- Disable the cell's two most critical tumor suppressor pathways (p53 and pRb)
- Prevent DNA repair and apoptosis
- Drive uncontrolled proliferation
- Promote accumulation of genetic alterations and chromosomal instability (50,52).

In feline models, these interactions have been validated through molecular and biochemical analyses, Altamura et al. (44) showed that FcaPV-2 E6 forms a complex with feline E6AP, enhancing p53 degradation. In parallel, E7 was shown to indirectly up-regulate p16(INK4a), consistent with pRb pathway disruption, and p16 over-expression has been reported in FcaPV-positive SCC (38,40).

The result of these interactions is deregulated cell cycle progression, resistance to apoptosis and enhanced cellular proliferation, setting the stage for malignant transformation (47).

3.3.2 Molecular mechanisms of virus-host interaction

Beyond direct effects on the cell cycle, PV modulate several host processes to facilitate immune evasion, persistent infection and tumor progression (30,51).

- Immune evasion: PV can downregulate MHC class I expression on infected keratinocytes, impairing antigen presentation and cytotoxic T-cell recognition. They may also inhibit interferon signaling and alter the tumor microenvironment (TME) to suppress host immune responses (43).
- Inflammation and chronicity: persistent low-grade inflammation, often associated with chronic viral infection, can contribute to carcinogenesis by promoting oxidative stress and enhancing the survival of dysplastic clones (53). Chronic inflammation also amplifies EMT-related pathways via cytokines such as IL-6 and TNF- α (54).
- Induction of epithelial-mesenchymal transition (EMT): emerging evidence suggests that PV oncogenes may also activate EMT-related pathways. Studies in both humans and animals have shown that PV-positive tumors frequently exhibit loss of epithelial markers and gain of mesenchymal markers, as well as up-regulation of transcription factors such as TWIST-1, Snail and ZEB1 (13,16).
- Activation of oncogenic signaling pathways: in equine SCC associated with EcPV2, viral infection correlates with activation of the Wnt/ β -catenin pathway and increased expression of downstream effectors like LEF1 and FOSL1 (55,56). A similar mechanism may be operative in feline PV-associated SCC, although further investigation is needed.

3.4 Experimental and clinical evidence of the FcaPV-SCC association

A growing body of evidence supports the association between FcaPV, particularly FcaPV-2 and FcaPV-4, and the development of squamous cell carcinoma in cats. This association is not merely based on the detection of viral DNA, but also on the demonstration of viral gene transcription, the presence of viral oncoproteins and the identification of virus-induced molecular alterations within neoplastic tissues (49). These changes are strikingly similar to the oncogenic pathways observed in HPV-induced head and neck squamous cell carcinoma (HNSCC) in humans (11,17,34,52).

FcaPV DNA has been frequently detected in feline SCC, particularly those arising in UV-protected areas such as the oral cavity, perineum and subungual regions, and occasionally the nasal planum (3). In these locations, PCR and ISH have consistently identified the presence of FcaPV-2 and FcaPV-4 DNA in neoplastic tissues, suggesting a causal rather than incidental role (11,41).

In addition to invasive SCC, FcaPV has also been associated with precursor lesions. A recent case series described seven feline oral in situ carcinomas harbouring papillomavirus DNA (57). This finding expands the spectrum of FcaPV-related epithelial lesions and closely parallels the concept of intraepithelial neoplasia described in HPV-associated human pathology.

Crucially, active viral transcription has been demonstrated by reverse quantitative PCR (RT-qPCR), RNA ISH, and RNAscope, showing expression of E6 and E7 oncogenes within tumor cells. These findings indicate not only the presence of the virus, but also its biological activity in driving tumorigenesis (40).

One of the most reproducible molecular hallmarks of FcaPV-associated SCC is the over-expression of the tumor suppressor p16(INK4a), commonly interpreted as a surrogate marker of pRb inactivation due to E7 expression. This pattern parallels that observed in high-risk HPV-driven human SCC, particularly in the oropharynx and cervix, and serves as an important diagnostic clue in veterinary oncology (54,58,59).

SCC in cats represent a clinically relevant model for investigating the oncogenic mechanism of PV. Although the ethical limitations of experimental viral inoculation in live animals restrict in vivo studies, ex vivo investigations using PV-positive feline tumor tissues or derived cell line have demonstrated that expression of viral oncogenes, in particular E6 and E7, leads to key molecular alterations such as loss of p53 function and inactivation of the pRb, resulting in evasion of apoptosis and uncontrolled cell proliferation (44,47).

These findings align with evidence from equine SCC associated with EcPV2, where similar dysregulation of cell cycle and induction of EMT have been observed (16). Furthermore, these mechanisms are highly conserved in human oncology, where, especially HPV-16, drive the development of HNSCC through analogous molecular pathways (50,60). Together, this interspecies consistency supports the utility of feline SCC as a One Health-oriented comparative model for studying papillomavirus-induced epithelial carcinogenesis.

4 – EPITHELIAL-MESENCHYMAL TRANSITION

4.1 Definition and biological relevance of EMT

Epithelial-mesenchymal transition (EMT) is a dynamic and reversible biological process by which epithelial cells lose their characteristic polarity and intercellular adhesion, acquiring a mesenchymal phenotype with enhanced migratory and invasive capacities. This transition plays a critical role in embryonic development, wound healing, tissue regeneration and tumor progression (61,62).

During EMT epithelial cells down-regulate junctional proteins such as E-cadherin, a key component of adherens junctions, and up-regulate mesenchymal markers including vimentin and N-cadherin. These changes are accompanied by cytoskeletal remodelling, loss of apical-basal polarity and acquisition of spindle-shaped morphology (63).

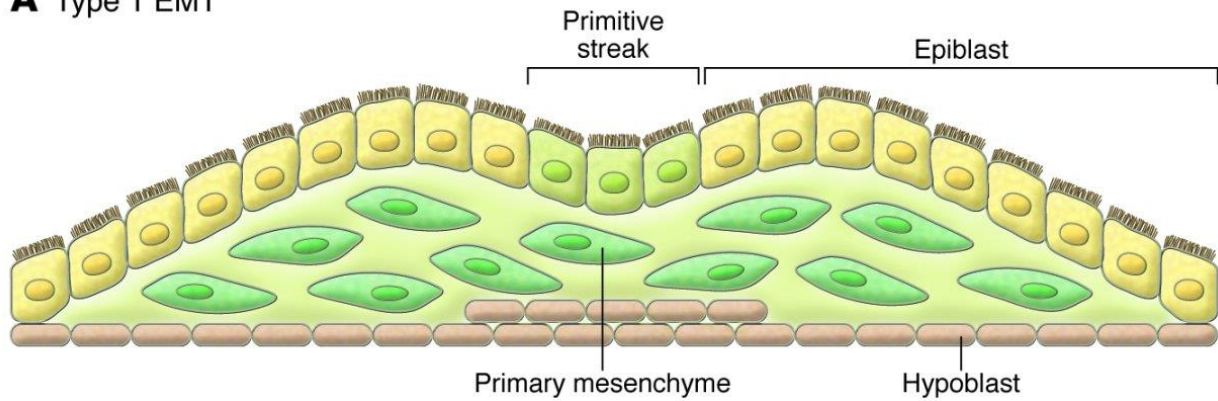
EMT is orchestrated by a set of transcription factors, including Snail, Slug, Twist, ZEB1 and ZEB2, which suppress epithelial gene expression and activate mesenchymal programs. These factors are regulated by multiple signaling pathways such as TGF- β , Wnt/ β -catenin, Notch and MAPK/ERK, integrating environmental stimuli into transcriptional reprogramming (62).

Three types of EMT are currently recognized based on context (Fig.1):

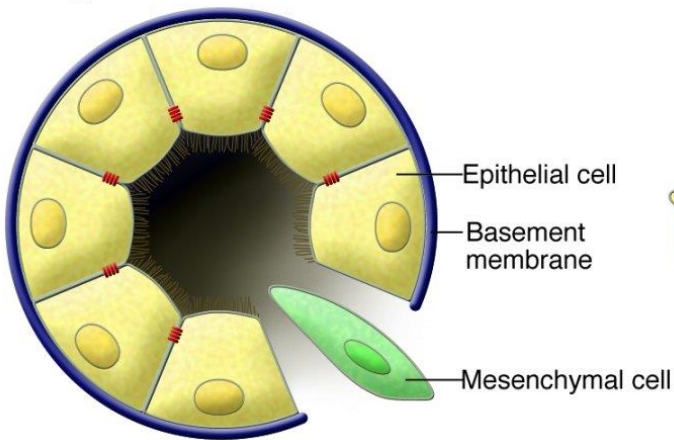
- Type 1. Occurs during embryogenesis and organ development
- Type 2- Involved in wound healing, tissue fibrosis and inflammation
- Type 3. Associated with epithelial tumor progression and metastasis (61).

In the oncologic context, type 3 EMT is of particular interest, as it enables carcinoma cells to invade the extracellular matrix, resist apoptosis and disseminate via lymphatic or hematogenous routes. Furthermore, EMT has been implicated in the acquisition of cancer stem cell-like properties and chemoresistance, posing significant challenges for therapeutic management (22,62).

A Type 1 EMT



B Type 2 EMT



C Type 3 EMT

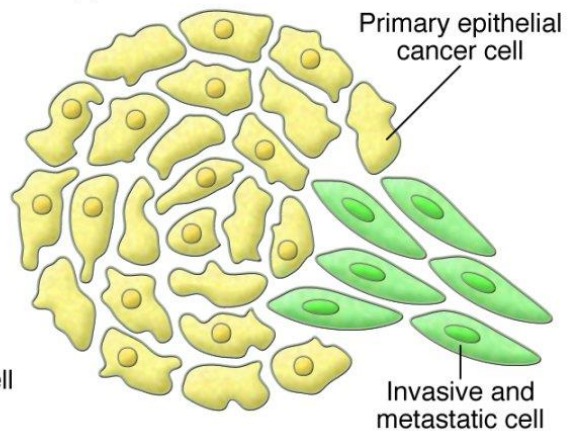


Figure 1. Schematic representation of the three types of epithelial–mesenchymal transition (EMT) (61).

4.2 EMT in embryonic life

EMT is a fundamental process during embryogenesis, where it orchestrates the formation of multiple tissue layers, organ and complex anatomical structures. This physiological EMT, also referred to as type 1 EMT, is tightly regulated and transient, ensuring tissue remodelling without malignant transformation (63,64).

One of the earliest and most well-characterized examples of EMT during development occurs during gastrulation, when a single-layered epiblast gives rise to the mesoderm and endoderm. In this context, epithelial cells lose their apico-basal polarity and intercellular adhesion and acquire migratory capacity to populate deeper embryonic layers (64,65). Later in development, EMT is critical during neural crest formation. Neural crest cells originate at the border between the neural plate and the non-neural ectoderm and undergo EMT to delaminate from the neuroepithelium and migrate to different sites, where they differentiate into melanocytes, craniofacial cartilage,

peripheral neurons and glial cells (66). This process involves a finely tuned regulation of transcription factors such as Snail, Slug, Twist and ZEB, which repress epithelial markers and activate mesenchymal genes (67).

Additional developmental events requiring EMT include:

- Heart valve formation. During early cardiac development cells lining the inner surface of the embryonic heart undergo EMT in response to molecular signals from the adjacent myocardium. These endocardial cells lose their epithelial characteristics and migrate into the surrounding extracellular matrix to form a specialized mesenchymal tissue known as the endocardial cushion. This mesenchymal population later contributes to the development of cardiac valves and septa (63,68).
- Palate fusion. During the formation of the secondary palate, the two palatal shelves must fuse to form a continuous structure. For this fusion to occur, cells in the medial epithelial seam must be eliminated. One mechanism by which this occurs is EMT. The seam epithelial cells transition into mesenchymal-like cells, allowing them to integrate into the surrounding palatal mesenchyme and thereby complete the fusion process. This EMT event is critical to prevent cleft palate malformations (63,69).
- Somite differentiation. Somites are segmented blocks of mesoderm located on either side of the developing neural tube. The ventral portion of the somite (sclerotome) undergoes EMT to give rise to migratory mesenchymal cells that contribute to the formation of the vertebral column and rib cartilage. Meanwhile, the dermomyotome gives rise to skeletal muscle and dermis (61,63).

4.3 EMT in wound healing, tissue fibrosis and inflammation

Beyond embryogenesis, EMT plays a role in post-natal tissue repair and remodelling. This physiological and transient EMT is known as Type 2 EMT and it's activated in response to tissue injury, inflammation and fibrotic stimuli (61).

4.3.1 EMT in wound healing

Following epithelial injury, such as skin abrasion or mucosal ulceration, epithelial cells at the wound edge undergo partial EMT. They downregulate adhesion molecules like E-cadherin, loosen intercellular junctions and adopt a migratory phenotype, allowing them to cover the wound bed through re-epithelialization (65). This process is reversible and epithelial integrity is restored via mesenchymal-epithelial transition (MET) once wound closure is achieved (70).

During tissue repair EMT is activated to promote cell migration and regeneration. This process is regulated by several key molecular signals present in the wound microenvironment (61). The most important regulators include:

- Transforming growth factor-beta (TGF- β). Is considered the central inducer of EMT in wound healing. It is secreted by platelets, macrophages and damaged epithelial cells at the site of injury. Once released, TGF- β binds to its receptors on epithelial cells, triggering a cascade of intracellular signals that lead to down-regulation of epithelial markers and activation of mesenchymal genes (62).
- Hypoxia-inducible factor 1-alpha (HIF-1 α). In injured tissues oxygen levels are often reduced, creating a hypoxic microenvironment. In response, cells stabilize and activate HIF-1 α , a transcription factor that helps them adapt to low oxygen conditions. HIF-1 α can directly or indirectly promote EMT by enhancing the expression of genes like Twist1 which facilitates cell migration and survival under stress (62).
- Reactive oxygen species (ROS) and pro-inflammatory cytokines. After injury the inflammatory response produces ROS and cytokines such as interleukin-6 (IL-6) and tumor necrosis factor-alpha (TNF- α). These molecules activate intracellular signalling pathways which in turn boost the transcription of EMT drivers (Snail, TWIST-1, ZEB1) and contribute to epithelial junction disruption and cytoskeletal reorganization facilitating cell motility (62).

4.3.2 EMT in fibrosis

EMT is physiological during wound healing, but in the context of chronic injury or persistent inflammation it can become pathological. When tissue damage is not resolved, epithelial cells exposed to prolonged stress signals may undergo sustained EMT, transitioning into myofibroblasts,

specialized contractile cells involved in fibrotic remodelling (71). These EMT-derived myofibroblasts are characterized by loss of epithelial markers, gain of mesenchymal and contractile proteins, increased secretion of extracellular matrix (ECM) components. The accumulation of ECM leads to tissue stiffening, loss of normal architecture and progressive organ dysfunction (71,72).

In chronic kidney disease (CKD), renal tubular epithelial cells exposed to TGF- β and inflammatory cytokines can undergo partial or full EMT, contributing to the expansion of interstitial fibroblast-like cells. These cells secrete ECM proteins that replace functional nephrons with fibrotic scar tissue, impairing filtration capacity (72,73).

In idiopathic pulmonary fibrosis (IPF), alveolar epithelial cells are repeatedly injured and may undergo EMT in response to oxidative stress and fibrogenic cytokines. This leads to the accumulation of fibroblastic foci in the lung parenchyma, resulting in progressive respiratory failure due to reduced elasticity and gas exchange (71,74).

In the liver, hepatocytes and cholangiocytes can undergo EMT under chronic inflammatory conditions, such as viral hepatitis or biliary obstruction. These cells contribute to portal and perisinusoidal fibrosis, altering hepatic microarchitecture and leading to cirrhosis and portal hypertension (75).

4.3.3 EMT and inflammation

Chronic inflammation is a powerful driver of EMT in both fibrotic and pre-neoplastic contexts. Unlike the tightly regulated and transient EMT observed in wound healing, persistent inflammatory signals can sustain a pro-EMT microenvironment, disrupting epithelial homeostasis over time (76).

Long term inflammation leads to the continuous production of cytokines and growth factor, in particular transforming growth factor- β 1 (TGF- β 1), interleukin-1 β (IL-1 β) and interleukin-6 (IL-6), tumor necrosis factor- α (TNF- α). These cytokines repress epithelial markers and activate mesenchymal genes, pushing epithelial cells toward and more motile, invasive phenotype (62,65).

Immune cells recruited during chronic inflammation contribute to EMT through paracrine signalling and extracellular matrix remodelling. Macrophages secrete matrix metalloproteinases (MMP-2 and MMP-9) that degrade the basement membrane and facilitate epithelial detachment, they also produce ROS and nitric oxide which induce DNA damage and oxidative stress (63,76).

Persistent EMT in an inflamed microenvironment not only promotes fibrosis, but may also set the stage for neoplastic transformation. In tissues subjected to repetitive injury and repair cycles prolonged EMT leads to genomic instability, evasion of apoptosis, loss of epithelial polarity and cohesion, acquisition of stem-like and invasive properties typical of malignant cells (53,77).

This transition is particularly well-documented in human medicine, where EMT plays a critical role in the progression of carcinomas arising in chronically inflamed tissue. Notable examples include colitis-associated colorectal cancer, hepatocellular carcinoma developing in cirrhotic livers and lung adenocarcinoma arising in fibrotic pulmonary tissue (53,75,78).

4.4 EMT in epithelial tumors

4.4.1 Molecular mechanisms

In epithelial tumors the reactivation of EMT represents a mechanism for tumor progression, invasion and metastasis. Unlike the transient and reversible EMT observed during development or wound healing, EMT in neoplastic contexts (Type 3 EMT) is often persistent, only partially reversible and associated with poor prognosis (65,77).

The molecular mechanism of EMT in tumors is orchestrated by a network of signalling pathways, transcription factors and epigenetic regulators, which converge to repress epithelial identity and promote mesenchymal traits (62):

- TGF- β pathway. Acts as a central inducer of EMT in tumor cells, activates the SMAD complex, leading to transcription of EMT-promoting genes like Snail, TWIST and ZEB1/2 (62).
- Wnt/ β -catenin pathway. Stabilization and nuclear translocation of β -catenin promotes transcription of mesenchymal genes and enhances cell migration and invasion (62).

- Notch and Hedgehog pathway. Contribute to EMT induction and the acquisition of stem cell-like features (65).
- NF- κ B and IL-6/STAT3 signalling. Often activated in tumor-associated inflammation promoting EMT and cell survival under stress conditions (53).

EMT is primarily driven by transcriptional repressors of epithelial markers and inducers of mesenchymal phenotype. Snail and Slug repress E-cadherin and induce vimentin and fibronectin, TWIST promote cell motility and mesenchymal identity, ZEB1 and ZEB2 suppress epithelial polarity and cell adhesion genes. These transcription factors are often co-regulated by oncogenic stimuli, inflammatory cytokines and hypoxia (62,65).

4.4.2 Role in tumor progression, invasion and metastasis

In epithelial tumors the activation of EMT confers a set of phenotypic and functional alterations that significantly enhance tumor aggressiveness. These changes are central to the invasive, metastatic, immune-evasive and therapy-resistant behaviour of many carcinomas (77,79).

One of the hallmark effects of EMT is the loss of epithelial cell-cell adhesion, mainly due to down-regulation of E-cadherin, a critical component of adherens junctions. Simultaneously, tumor cells up-regulate mesenchymal markers like N-cadherin, vimentin and fibronectin, which facilitate cytoskeletal reorganization and motility. This transition enables epithelial cancer cells to break through the basement membrane and invade surrounding stroma (62,65).

Transcription factors activated during EMT, such as Snail and TWIST, up-regulate anti-apoptotic signalling pathways that allow epithelial-derived tumor cells to evade anoikis, a form of programmed cell death induced by loss of adhesion to the extracellular matrix. This survival mechanism is critical for enabling tumor cell dissemination through vascular or lymphatic routes (61,77).

EMT can also facilitate escape from immune surveillance by reducing expression of MHC class I molecules and tumor antigens, increasing secretion of immunosuppressive cytokines, recruiting

regulatory T cells and M2 macrophages to the tumor microenvironment. This immune modulation contributes to tumor persistence (53,80).

Through EMT, carcinoma cells gain the ability to invade vasculature, survive under anchorage-independent and hypoxic conditions in circulation and extravasate into distant tissue (Fig. 2). At secondary sites, many tumor cells undergo mesenchymal-epithelial transition (MET) to re-establish proliferative epithelial colonies, completing the metastatic cascade (65,77).

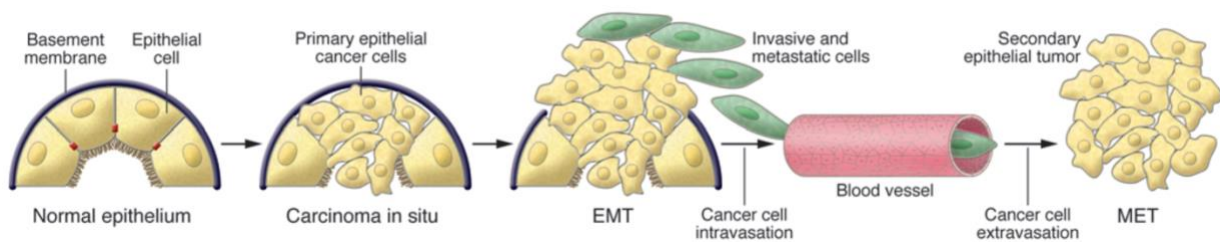


Figure 2. Contribution of EMT to metastatic competence (61)

4.4.3 EMT and therapeutic resistance

The activation of EMT is increasingly recognized not only as a driver of invasion and metastasis, but also as a key contributor to resistance against conventional tumor therapies, including chemotherapy, radiotherapy and targeted agents (81,82).

During EMT, epithelial tumor cells undergo transcriptional and phenotypic reprogramming that results in the acquisition of mesenchymal traits such as increased motility, resistance to apoptosis, reduced proliferation, metabolic plasticity and a capacity to survive under stress. These features collectively impair the efficacy of treatments that preferentially target rapidly dividing, epithelial like cells (61,62).

Several mechanisms link EMT to therapeutic resistance:

- Anti-apoptotic signalling. EMT-associated transcription factors such as Snail, TWIST-1 and ZEB1 activate survival pathways, reducing treatment-induced apoptosis (83,84).
- Anoikis resistance. Cells undergoing EMT become resistant to anoikis, allowing survival during detachment and dissemination (66).

- Cancer stem-like properties. EMT has been shown to induce cancer stem cell phenotypes, which are intrinsically resistant to DNA-damaging agents and contribute to tumor relapse and heterogeneity (85,86).
- Altered cell cycle and metabolic state. EMT shifts cells into a slow-cycling, metabolically adaptive state, rendering them less sensitive to treatments targeting proliferative cells (82,87).

In HPV-associated tumors, such as cervical tumor or head and neck squamous cell carcinoma (HNSCC), EMT has been implicated in resistance to chemoradiotherapy. Tumors with high expression of mesenchymal markers or EMT transcription factors such as TWIST-1 or ZEB1 often exhibit poor treatment response and early recurrence (70,88,89).

In the feline model, although mechanistic studies directly linking EMT to treatment failure are limited, available immunohistochemical data provide compelling indirect evidence. Harris et al. (13) demonstrated that feline oral SCC exhibit variable expression of EMT markers, including loss of E-cadherin, gain of vimentin and nuclear localization of TWIST-1, particularly in poorly differentiated and recurrent tumors, suggesting a link between EMT activation and aggressive clinical behaviour. Moreover, a recent clinical study on electrochemotherapy in feline nasal planum SCC (9) reported that tumors with incomplete response or early recurrence frequently displayed mesenchymal-like morphology and cytoskeletal reorganization, further supporting the role of EMT in therapeutic resistance.

Additionally p16(INK4a) over-expression, often associated with PV-driven tumorigenesis, has been observed in feline SCC with mesenchymal phenotypes (11), hinting at a combined role of viral oncogenesis and EMT in shaping tumor plasticity and treatment failure.

Understanding the link between EMT and therapeutic resistance has important implications for personalized oncology, both in human and veterinary medicine. Biomarkers such as E-cadherin loss, vimentin expression or p16 over-expression may help stratify patients for more aggressive or alternative treatments (11,87). Moreover, targeting EMT-inducing pathways is being explored as a novel therapeutic strategy to overcome resistance and prevent metastasis (62,90).

4.5 EMT molecular markers

The EMT is characterized by a coordinated shift in the expression of specific molecular markers, reflecting the loss of epithelial traits and the acquisition of mesenchymal features. These markers are routinely used in both experimental and diagnostic settings to identify EMT activation and to correlate it with tumor progression, invasiveness and prognosis (61,62,65).

4.5.1 Epithelial markers

During the activation of EMT, epithelial cells progressively lose key features such as cell-cell adhesion, apico-basal polarity and cytoskeletal organization, going toward a more migratory and invasive phenotype. This process is associated with the down-regulation of epithelial markers, which serve as critical indicators of EMT status in both experimental and diagnostic pathology (62,65).

E-cadherin is a calcium-dependent transmembrane glycoprotein and a core component of adherens junctions. It plays a fundamental role in maintaining epithelial architecture by stabilizing intercellular contact and preserving tissue polarity. During EMT, CDH1 expression is repressed by EMT-inducing transcription factors such as Snail, Slug and ZEB1/2. Loss of E-cadherin weakens epithelial cohesion and facilitates detachment and invasion, making it a hallmark of EMT and a predictor of tumor aggressiveness and metastatic potential (13,62,65).

A critical event during EMT is the so-called “cadherin switch”, a process by which epithelial cells down-regulate E-cadherin and simultaneously up-regulate N-cadherin, a cadherin isoform typically expressed in mesenchymal and neural tissues. This switch, regulated by EMT-transcription factors such as Snail, TWIST-1 and ZEB1, has biological implications, in fact while E-cadherin forms stable, high affinity cell-cell adhesions that preserve epithelial integrity, N-cadherin mediates weaker, more dynamic adhesions that are permissive to cell movement and collective migration (91).

The “cadherin switch” not only facilitates detachment from the primary tumor mass, but also promotes interactions with stromal and endothelial cells, enhancing tumor cells invasiveness and intravasation. This phenomenon, often described as “N-cadherin-mediated motility” is considered

a functional hallmark of EMT and has been correlated with poor prognosis and increased metastatic potential in several human carcinomas (92,93).

Cytokeratins (CK) are intermediate filament proteins characteristic of epithelial cells, they support structural integrity and cytoskeletal organization. EMT is commonly associated with loss of expression of certain CK subtypes, in particular CK8 and CK18, or cytoskeletal reorganization, reflecting the transition to a mesenchymal phenotype (13,61,63).

Tight junction components such as claudin-1, occluding and zonula occludens-1 (ZO-1) are crucial for maintaining epithelial barrier integrity. Their expression is frequently down-regulated during early EMT, contributing to the disruption of cell polarity and increased paracellular permeability. Although not routinely evaluated in feline pathology, tight junction markers are widely studied in human and murine models as early indicators of EMT induction (65,84).

4.5.2 Mesenchymal markers

The EMT is characterized by the acquisition of mesenchymal features that provide epithelial-derived cells with increased plasticity, motility and invasiveness. This phenotypic reprogramming is accompanied by the up-regulation of mesenchymal markers, many of which play functional roles in cytoskeletal remodelling, extracellular matrix interaction and migratory behaviour (61,62,65,82).

N-cadherin is a calcium-dependent cell adhesion molecule normally expressed in neural and mesenchymal tissues. Its expression is typically low or absent in epithelial cells but becomes up-regulated during EMT in a process known as the “cadherin switch”, documented in both human carcinomas (e.g. breast, prostate, HNSCC) and companion animal tumors. This switch is not merely a passive marker of phenotype change, but an active driver of tumor progression. N-cadherin forms weaker more dynamic cell-cell contacts compared to E-cadherin and promotes interactions with fibroblast, endothelial cells and components of the extracellular matrix, facilitating cell migration and tissue invasion (91–93).

This switch is often mediated by EMT-associated transcription factors such as Snail, TWIST-1 and ZEB1, which not only repress CDH1, but also transcriptionally activate CDH2, encoding N-cadherin. In several human tumors, including breast and lung squamous carcinomas, increased N-cadherin expression is correlated with high-grade histology, lymphovascular invasion, metastasis and poor patient outcome (89,92,93).

Vimentin is an intermediate filament protein that is widely considered one of the most reliable and conserved markers of mesenchymal phenotype. It supports cytoskeletal reorganization, cell elongation and mechanical resilience, which are necessary for mesenchymal migration. Vimentin expression increases during EMT, contributing to changes in cell shape and promoting interactions with integrins and focal adhesions (13,61). In human oncology vimentin is overexpressed in a variety of aggressive tumors, including squamous cell carcinomas, sarcomas and triple-negative breast cancers, and it's associated with invasiveness and poor prognosis (94).

Fibronectins are glycoproteins that connect cells with collagen fibers in the extracellular matrix (ECM), allowing cells to move through the ECM. They play an important role in matrix remodelling, cell adhesion and migration by binding integrins. During EMT fibronectin expression is transcriptionally up-regulated by TGF- β signalling and EMT transcription factor such as Snail and ZEB1. It supports the migratory capacity of EMT-transformed cells and contributes to pre-metastatic lesions formation (63,71).

α -smooth muscle actin (α -SMA) is a cytoskeletal contractile protein typically expressed in smooth muscle cells and myofibroblasts. In EMT contexts is particularly relevant in fibrosis, wound healing and tumors with myofibroblastic differentiation. Its co-expression with vimentin and loss of E-cadherin strongly suggests a mesenchymal shift (71,72).

β -catenin plays a dual role in epithelial homeostasis and EMT. Under physiological conditions, it forms part of the E-cadherin-catenin complex at adherens junctions, anchoring the actin cytoskeleton to the plasma membrane and maintaining epithelial polarity. During EMT, loss of E-cadherin leads to the dissociation of this complex and frees β -catenin, which can translocate to the nucleus. In the nucleus, β -catenin acts as a transcriptional co-activator in the Wnt signalling

pathway, promoting the expression of mesenchymal genes and EMT-regulating transcriptional factors such as Snail and TWIST (62,95).

4.5.3 Transcription factors

The induction of EMT is orchestrated by a set of transcription factors that act as master regulators of the process. Among these, the Snail, TWIST and ZEB families are the most extensively studied. These transcription factors repress the expression of epithelial markers, particularly CDH1 and activate mesenchymal gene programs promoting a motile, invasive and therapy-resistant phenotype (65,82,84).

Snail and Slug are transcriptional repressors encoded by SNAI1 and SNAI2 genes respectively. They play a role in initiating EMT by binding to E-box elements in the CDH1 promoter and repressing E-cadherin transcription. Snail1 expression is regulated by multiple signalling pathways including TGF- β , NF- κ B, Wnt/ β -catenin, ROS and hypoxia (62,65). Snail proteins also repress other epithelial junction proteins such as claudins, occludins, cytokeratins and mucins (84).

TWIST-1 is a transcription factor that binds to E-box sequences and induce EMT through both direct and indirect mechanisms: represses CDH1 and enhances mesenchymal gene expression, while also up-regulating Snail1 and Snail2, thus amplifying EMT signalling (96). TWIST-1 acts as a hypoxia-responsive EMT regulator, with HIF-1 α mediated transcriptional activation observed in multiple carcinomas (83,96).

ZEB1 and ZEB2 are transcriptional repressors that also bind to E-box sequences in the CDH1 promoter, directly inhibiting E-cadherin transcription. ZEB factors repress epithelial genes and activate mesenchymal markers (82). Unlike TWIST-1, ZEB proteins are also strongly involved in immune evasion, stemness and epigenetic reprogramming (82,97).

Hypoxia-inducible factor 1-alpha (HIF-1 α) is a master regulator of the cellular response to low oxygen levels and plays a critical role in promoting EMT under hypoxic conditions. Stabilized in hypoxic tumor microenvironments, HIF-1 α translocates to the nucleus and activates a transcriptional program that enhances cellular survival, angiogenesis and invasiveness (98). HIF-

1 α directly or indirectly up-regulates EMT-inducing transcription factors such as TWIST-1, Snail and ZEB1 and promotes mesenchymal gene expression, including vimentin, fibronectin and matrix metalloproteinases (MMP) (96,99).

Although much of this evidence is derived from human studies, immunohistochemical expression of Snail and TWIST-1 has been observed in feline and equine SCC, particularly in tumors with invasive behaviour and FcaPV or EcPV2 association, highlighting their translational relevance (13,16,37).

5 – INTERPLAY BETWEEN PVs AND EMT

5.1 Viral oncoproteins as inducers of EMT

The molecular interplay between viral oncogenes and EMT has emerged as a central theme in the pathogenesis of virus-induced epithelial tumors. Several DNA tumor viruses, including “high-risk” HPV, have been shown to manipulate host transcriptional programs and epigenetic regulators to induce EMT. This reprogramming facilitates not only cellular transformation, but also immune evasion, tissue invasion and metastatic dissemination (90).

Viral oncoproteins such as E6 and E7 play a central role by disrupting critical tumor suppressor pathways, including p53 and pRb, and simultaneously activate cellular signalling cascades that promote EMT (100). These pathways include TGF- β /SMAD, Wnt/ β -catenin, NF- κ B, PI3K/AKT, MAPK/ERK and hypoxia/HIF-1 α , all of which converge on transcriptional regulators such as Snail, TWIST-1 and ZEB (62,65,101).

E6 promotes proteasomal degradation of p53 through recruitment of the E6-associated protein ubiquitin ligase, while E7 binds and inactivates the pRb, liberating E2F transcription factors and driving cell cycle progression (100). In addition to these canonical roles, both proteins have been shown to modulate EMT-related pathway: E6 suppresses E-cadherin through TGF- β signalling and β -catenin activation, E7 enhances expression of mesenchymal genes via PI3K/AKT and MYC pathways (87,100).

In feline SCC, FcaPV-2 E6 and E7 oncoproteins have been shown to possess transforming activity both in vitro and in vivo. In feline keratinocyte-based models, E6 enhances the activation of mitogen-activated protein kinase (MAPK) and protein kinase B (AKT/PKB) signalling pathways, two major cascades involved in cell proliferation, mediated by epidermal growth factor receptor (EGFR) over-expression, highlighting a virus-specific mechanism of signal transduction (102).

The same group also demonstrated that FcaPV-2 E6 physically interacts with E6AP, an E3 ubiquitin ligase, facilitating the degradation of the p53 tumor suppressor via the proteasome pathway. This event not only removes a key apoptotic checkpoint, but also contributes to the deregulation of genes involved in cellular motility and invasion. The loss of p53, combined with pRb inactivation

by E7, sets the stage for EMT by releasing the repression of EMT transcription factors such as Snail, TWIST-1 and ZEB1 (44).

Beyond these canonical interactions, viral oncoproteins are increasingly recognized as modulators of EMT through activation of TGF- β signalling. Transforming TGF- β is a master inducer of EMT in epithelial tumors and can be up-regulated either directly by viral proteins or indirectly via alterations in the tumor microenvironment. TGF- β signalling activates SMAD-dependent transcriptional programs that suppress epithelial markers and induce mesenchymal genes, promoting a migratory and invasive phenotype (103,104).

Additionally, the AKT pathway, activated by FcaPV-2 E6, has been implicated in the stabilization of EMT transcription factors and in promoting resistance to apoptosis and anoikis, both of which are hallmarks of EMT-associated tumor progression. The MAPK/ERK pathway, also activated in vitro by FcaPV-2, contributes to EMT by enhancing cellular motility, cytoskeletal remodelling and the expression of MMP, which facilitate extracellular matrix degradation and invasion (49,102).

5.2 Evidence from human medicine: HPV-induced EMT in HNSCC

The oncogenic potential of high-risk human papillomaviruses (HR-HPV), particularly HPV-16 and HPV-18, has been extensively studied in cervical cancer and in head and neck squamous cell carcinoma (HNSCC), where these viruses are etiologically implicated in a substantial subset of cases. Accumulating evidence suggests that HPV-driven carcinogenesis is tightly linked to the activation of EMT, particularly in advanced or metastatic tumors (90,105,106).

The viral oncoproteins E6 and E7 play a central role in this process. Beyond their canonical functions, i.e. degradation of p53 and inactivation of pRb, they have been shown to interact with multiple host cell signalling pathways that directly or indirectly induce EMT (87,100).

These include: TGF- β /SMAD, which cooperates with E6 to repress E-cadherin expression (87), PI3K/AKT and Wnt/ β -catenin, both activated by E7 and involved in mesenchymal gene expression (86), NF- κ B contributing to inflammation-driven EMT in HPV-positive tumors (53).

Histopathological and molecular studies have consistently demonstrated that HPV-positive SCC, notably those of the cervix and oropharynx, exhibit distinct pattern of EMT compared to their HPV-negative counterparts (106–108). These tumors often display loss of epithelial characteristics, including down-regulation or delocalization of E-cadherin and cytokeratin, acquisition of mesenchymal traits such as increased expression of vimentin, N-cadherin and fibronectin, up-regulation of EMT-associated transcription factors, in particular TWIST-1, Snail and ZEB1, which are directly or indirectly modulated by E6/E7 oncoproteins (87,100,106).

This phenotypic shift correlates with clinically relevant tumor behaviours, including:

- Down-regulation of E-cadherin, a key adhesion molecule, is strongly associated with local invasiveness, loss of epithelial polarity and regional lymph node metastasis in cervical and oropharyngeal SCC (109,110).
- Overexpression of vimentin, a marker of mesenchymal differentiation, has been linked to enhanced migratory potential and early dissemination (111).
- TWIST-1, a central transcriptional driver of EMT, is frequently up-regulated in HPV-positive tumors, where it's associated with tumor progression, radio-chemoresistance and poor prognosis (112).

5.3 FcaPV and EMT: synergistic role in tumor progression

The oncogenic potential of FcaPV in the pathogenesis of feline SCC extends beyond the classical mechanisms of tumor initiation. Increasing molecular and histopathological evidence supports the concept that FcaPV not only contributes to neoplastic transformation through the inactivation of tumor suppressor pathways, but may also play a role in promoting EMT, thereby enhancing tumor progression, invasion and plasticity (11,13,34).

Building upon the well-established oncogenic mechanism of high-risk HPV in cervical carcinoma and HNSCC, recent veterinary research has begun to explore whether comparable molecular events occur in feline SCC associated with FcaPV infection (11,18,34). In human oncology, it is now widely accepted that HPV oncoproteins, especially E6 and E7, not only drive tumor initiation by inactivating tumor suppressors such as p53 and pRb, but also contribute to tumor progression by triggering EMT, a critical step in local invasion and metastasis (100,108).

Recent veterinary studies have uncovered that FcaPV-positive feline SCC exhibit:

- FcaPV DNA, particularly from FcaPV-2 and FcaPV-4, has been consistently detected in both cutaneous and mucosal SCC in cats (11,41,49).
- The transcriptional activity of viral oncogenes E6 and E7 has been demonstrated in SCC tissues, confirming active viral participation in tumor biology (34,47,49).
- Immunohistochemical analyses reveal clear features of EMT in FcaPV-positive SCC, including loss of E-cadherin, increased vimentin expression and nuclear up-regulation of EMT-related transcription factors such as TWIST-1 and ZEB1, particularly at the invasive tumor front (13,49).

One of the earliest and most consistent molecular clues supporting a functional role for viral oncogenes in feline SCC is the frequent over-expression of p16(INK4a), a surrogate marker of pRb pathway inactivation, which reflects the activity of E7 oncoprotein. While p16 itself is not a direct marker of EMT, its dysregulation is a hallmark of viral oncogenesis and often precedes or coexists with EMT induction (11,19).

Current data suggests that FcaPV oncoproteins not only initiate tumorigenesis, but also facilitate tumor progression through the activation of EMT-related signalling pathways including TGF- β /SMAD signalling, a primary driver of EMT in multiple carcinomas, PI3K/AKT, which promotes survival, plasticity and resistance to anoikis, Wnt/ β -catenin, which enhances stemness, invasiveness and transcriptional reprogramming (11,13,34).

Furthermore, the tumor microenvironment, rich in pro-inflammatory cytokines (e.g. IL-6, TNF- α), hypoxia and TGF- β , likely amplifies this process, creating a feed-forward loop in which EMT further destabilizes the genome, enhances cellular plasticity and facilitates both local invasion and distant dissemination (6,13).

This pathogenic model is not unique to feline oncology, but mirrors the molecular dynamics observed in HPV-driven cervical tumor and HNSCC in humans (90,108), and EcPV2-associated SCC in horses, where EMT features are similarly associated with aggressive tumor behaviour (16,55,56).

5.4 Comparative oncology: insights from canine, equine and human SCC model

By examining SCC in companion animals and humans, shared pathogenic mechanisms, such as viral oncogene-mediated transformation, cell cycle deregulation and EMT, can be identified, reinforcing a One Health approach to oncologic research.

In horses, *Equus caballus* papillomavirus type 2 (EcPV2) has been definitively implicated in the pathogenesis of SCC of the larynx, penis, prepuce and vulva. Like its human and feline counterparts, EcPV2 encodes E6 and E7 proteins that inactivate p53 and pRb tumor suppressor pathways, promote cell cycle deregulation and are increasingly recognized as inducers of EMT (15,55,56).

Recent studies have documented the expression of EMT markers in EcPV2-associated SCC, including down-regulation of E-cadherin, up-regulation of vimentin and N-cadherin and nuclear localization of transcription factors such as TWIST-1 and ZEB1 (15,16,55). These findings confirm the activation of EMT in naturally occurring equine SCC, especially at the invasive front of tumors. Moreover, De Paolis et al. (16) demonstrated strong EMT marker expression in a EcPV2-positive vulvar SCC in a mare, supporting the involvement of EMT in equine tumor progression. Similarly, Armando et al. (15) demonstrated EMT marker expression in a laryngeal SCC with EcPV2 DNA, linking viral infection to phenotypic plasticity and aggressiveness.

In addition, Yamashita-Kawanishi et al. (17) reported a well-characterized case of EcPV2-associated vulvar SCC in a Japanese mare, showing robust E6/E7 mRNA expression, high viral DNA load and nuclear p16 positivity, with minimal p53 degradation. These findings reflect a viral oncogenic mechanism partially overlapping to the classical HPV model observed in humans.

While EcPV-2 remains the most relevant genotype in equine SCC, recent evidence has shown that other papillomavirus types may also contribute to carcinogenesis, although with much lower frequency. In particular, EcPV-7 has been reported as a rare cause of penile squamous cell carcinoma, highlighting the need to consider viral diversity in equine oncogenesis (113).

In human medicine, the oncogenic role of high-risk HPV, particularly HPV-16 and HPV-18, in the development of cervical carcinoma and HNSCC is well-established (90). These viruses contribute to tumorigenesis primarily through the actions of the viral oncoproteins E6 and E7, which inactivate key tumor suppressors such as p53 and pRb, leading to cell cycle deregulation, inhibition of apoptosis and genomic instability (50,51). Beyond these classical mechanisms of carcinogenesis, an expanding body of literature demonstrates that HPV oncoproteins also play an active role in modulating the tumor microenvironment, facilitating EMT, a crucial process for tumor invasion, metastasis and therapeutic resistance (90,108).

HPV-positive tumors exhibit activation of several canonical EMT-associated signalling pathways, including TGF- β /SMAD, a master regulator of EMT that orchestrates transcriptional reprogramming toward mesenchymal phenotypes, Wnt/ β -catenin pathway, which promotes cellular plasticity, migration and stem-like properties, PI3K/AKT pathway, enhancing survival, anoikis resistance and metabolic adaptation (61,62,70). These pathways are not only activated by cellular stress and microenvironmental cues, but are directly modulated by E6 and E7 oncoproteins, creating a synergic effect that amplifies EMT induction (53,100).

Multiple histopathological and molecular studies have consistently demonstrated that HPV-positive SCC, particularly those of the oropharynx and cervix, exhibit:

- Down-regulation of epithelial markers, such as E-cadherin and cytokeratins, correlating with reduced cell-cell adhesion (61,62,110).
- Up-regulation of mesenchymal markers, including vimentin, N-cadherin and fibronectin, associated with enhanced motility and invasiveness (61,87).
- Increased nuclear expression of EMT transcription factors, such as Snail, TWIST-1 and ZEB1, particularly in tumor areas exhibiting invasion and metastasis (84,114,115).

This partial or full EMT phenotype is now recognized as a key determinant of local invasion, lymph node metastasis, resistance to radiotherapy and chemotherapy, which is more frequently observed in HPV-positive compared to HPV-negative tumors (61,62,82,116).

The role of PV in canine squamous cell carcinoma is far less defined and appears to diverge significantly from the pathogenic models observed in cats, horses and humans. While early studies

as Zaugg et al. (37) detected PV DNA in canine mucosal and cutaneous SCC, including novel viral types, subsequent research has raised doubts about the oncogenic potential and biological relevance of these findings.

For instance, Munday et al. (36) described multiple oral carcinomas in a dog associated with a novel papillomavirus; however, the study lacked evidence of viral transcriptional activity or functional interaction with host cell cycle regulators. Similarly, Sabattini et al. (38) showed that p16 immunostaining in canine SCC does not correlate with papillomaviral DNA, suggesting the absence of pRb inactivation by viral oncoproteins, a key hallmark of high-risk PV-driven oncogenesis.

Furthermore, Porcellato et al. (39) demonstrated that canine oral SCC do not show transcriptional activity of CPV1 and that dogs may not represent a suitable model for high-risk HPB-related oral tumor. No consistent EMT immunophenotype has been identified in canine SCC in association with PV infection and expression of transcriptional regulators such as TWIST-1, ZEB1 or Snail has not been reported in PV-positive cases.

Therefore, although PV DNA may occasionally be detected in canine SCC, the current evidence does not support a significant etiological or pathogenic role for PV in dogs. The canine model appears limited in its translational value for studying PV-induced EMT and SCC progression.

Recent comparative reviews (35,48,54,117) emphasize the molecular parallels between PV-associated neoplasms in humans, cats and horses, particularly in their shared oncogenic mechanisms and EMT induction. Altamura and Borzachiello (49) argued that feline SCC shares key features with high-risk HPV-driven tumors, suggesting a continuum in the interplay between viral oncogenes, host pathways and EMT programs. More recently, Tutu et al. (118) synthesized current advances in feline SCC, highlighting that EMT activation in cats, similar to humans, is modulated by a combination of viral activity, host susceptibility and microenvironmental influences rather than by viral status alone.

6 – RESEARCH AIMS AND OBJECTIVES

The overall aim of the present study was to investigate the molecular and immunohistochemical features of feline nasal planum squamous cell carcinoma, with particular emphasis on the role of FcaPV infection and its potential interaction with EMT, as a mechanism of tumor progression.

The specific objectives were:

- to detect and characterize the presence of FcaPV DNA in feline nasal planum SCC samples using polymerase chain reaction
- to assess the transcriptional activity of FcaPV infection through the evaluation of viral oncogene (E6 and E7) expression
- to evaluate the immunohistochemical expression of epithelial, mesenchymal, hypoxia-related and EMT-associated markers in feline nasal planum SCC
- to analyse potential associations between FcaPV infection status and EMT-related immunophenotypic features
- to interpret the results within a comparative oncology and One Health framework, drawing parallels with human HPV-associated head and neck squamous cell carcinoma and with PV-associated SCC in other animal species.

7 – MATERIALS AND METHODS

7.1 Case selection

A total of 50 cases of feline nasal planum squamous cell carcinoma (npSCC) and 10 negative controls were included in this study. Tumor samples were retrospectively selected from the formalin-fixed paraffin-embedded (FFPE) archives of the veterinary pathology unit of the Department of Veterinary Medicine of the University of Parma, the veterinary pathology unit of the Department of Veterinary Medicine of the University of Perugia and the Institute of Pathology of the University of Veterinary Medicine of Hannover. The inclusion criteria for npSCC cases were histological diagnosis consistent with SCC located at the nasal planum, with sufficient tissue available for further analyses.

Negative control tissues were obtained from the nasal planum of adult domestic cats without macroscopic cutaneous lesions, sampled during routine necropsies performed at the Department of Veterinary Medicine at University of Parma. Histological sections of these samples were carefully reviewed, and only those exhibiting normal epidermal and dermal architecture, without evidence of hyperplasia, dysplasia, inflammation or actinic damage, were included as negative controls.

7.2 Histological evaluations

All FFPE tissue samples were sectioned at 5 μm thickness and stained with Mayer's haematoxylin and eosin (HE) using standard protocols. Histological evaluation was performed to confirm the diagnosis of SCC in all tumor samples. The diagnosis was established based on morphological criteria and confirmed by at least one board-certified veterinary pathologist.

7.3 Immunohistochemistry

Immunohistochemical (IHC) analysis was performed on 5- μm FFPE sections using standard protocols. The following primary antibodies were employed: pan-cytokeratin AE1/AE3, vimentin, E-cadherin, N-cadherin, TWIST-1, ZEB1, β -catenin and HIF-1 α . Details regarding antibody sources, dilutions, antigen retrieval methods and incubations times are summarized in Table 1.

Table 1 Details of the antibodies used for immunostaining, including primary antibody, host species, clonality, epitope retrieval method, blocking serum, dilution of primary antibody, secondary antibody.

Target antigen	Antibody Details/Clone	Blocking Serum	Heat Induced Epitope Retrieval (HIER)	Primary Antibody Dilution	Secondary Antibody (1:200)
E-cadherin	Monoclonal mouse anti-human, IgG2a, clone 36/E-cadherin BD 610181 (BD transduction laboratories)	Goat	Microwave 400 W, 3 cycles, 5 min. each, sodium citrate buffer, pH 6.0	1:100	Biotinylated goat anti-mouse IgG (BA-1000-Vector Labs)
Pan-cytokeratin AE3/AE1	Monoclonal mouse anti-huma, IgG1 SC-81714 (Santa Cruz Biotechnology)	Goat	Microwave 400 W, 3 cycles, 5 min. each, sodium citrate buffer, pH 6.0	1:100	Biotinylated goat anti-mouse IgG (BA-1000-Vector Labs)
β -catenin	Polyclonal goat anti-human, IgG, AB0095-200 (Sicgen)	Rabbit	Microwave 400 W, 3 cycles, 5 min. each, sodium citrate buffer, pH 6.0	1:1300	Biotinylated rabbit anti-goat IgG (BA-1000-Vector Labs)
N-cadherin	Polyclonal rabbit anti-human, IgG, 22018-1-AP (Proteintech)	Goat	Microwave 400 W, 3 cycles, 5 min. each, sodium citrate buffer, pH 6.0	1:1300	Biotinylated goat anti-rabbit IgG (BA-1000-Vector Labs)
Vimentin	Monoclonal mouse anti-human IgG1, Clone V9 (Dako)	Goat	Microwave 400 W, 3 cycles, 5 min. each, sodium citrate buffer, pH 6.0	1:100	Biotinylated goat anti-mouse IgG (BA-1000-Vector Labs)
ZEB1	Polyclonal rabbit anti-human, IgG, LS-C31478 (LSBio)	Goat	Microwave 400 W, 3 cycles, 5 min. each, sodium citrate buffer, pH 6.0	1:200	Biotinylated goat anti-rabbit IgG (BA-1000-Vector Labs)
TWIST-1	Polyclonal rabbit anti-human, IgG, Orb329955 (Biorbyt)	Goat	Microwave 400 W, 3 cycles, 5 min. each, sodium citrate buffer, pH 6.0	1:800	Biotinylated goat anti-rabbit IgG (BA-1000-Vector Labs)
HIF-1 α	Polyclonal rabbit anti-human, IgG, NB100-449 (NovusBio)	Goat	Microwave 400 W, 3 cycles, 5 min. each, sodium citrate buffer, pH 6.0	1:1000	Biotinylated goat anti-rabbit IgG (BA-1000-Vector Labs)

After dewaxing-rehydration, antigen retrieval was carried out by dipping the sections in 0.01 M sodium citrate buffer, pH 6.0, and heating them in a microwave oven for 15 min at 400 W. The sections were incubated in 3% hydrogen peroxidase for 15 min to block endogenous peroxidase.

Incubation with primary antibody was carried out overnight at 4°C. After being washed twice in PBS, pH 7.4, the slides were incubated for 30 min with a biotinylated goat anti-rabbit, or a goat anti-mouse, or a rabbit anti-goat IgG antibody.

An avidin-biotin complex (ABC) peroxidase kit (Vectastain, Elite, ABC-Kit PK-6100, Vector Labs, Burlingame, CA, USA) was used after secondary antibody application. The immunolabeling was revealed with 3,3-diaminobenzidine tetrahydrochloride (DAB) chromogen system (DAB-Kit-SK4100, Vector Labs), and counterstaining was performed with Mayer's haematoxylin. Negative control sections were incubated with rabbit or goat isotype control antibody, using the same concentration of the primary antibody.

Slides were examined with Nikon Eclipse E800 microscope (Nikon Corporation, Minato-Ku, Japan) and pictures were obtained with a digital sight DS-Fi1 camera (Nikon Corporation, Minato-Ku, Japan).

The immunoreactivity of each marker was assessed semi-quantitatively based on intensity (0 = no immunolabeled cells, 1 = 1% to 25% of immunolabeled cells, 2 = 26% to 50% of immunolabeled cells, 3 = 51% to 75% of immunolabeled cells, 4 = 76% to 100% of immunolabeled cells). The subcellular localization of staining (nuclear, cytoplasmic or membranous) was also recorded for some of the marker (TWIST-1, ZEB1 and HIF-1 α).

7.4 DNA extraction and FcaPV detection

DNA extraction was performed from formalin-fixed paraffin-embedded (FFPE) tissue blocks using a combined manual and automated protocol to ensure optimal recovery and purity of nucleic acids. The extraction process was carried out using the QIAamp DNA FFPE Advanced Kit (Qiagen, Hilden, Germany), with partial automation on the QIAcube[®] extraction platform (Qiagen, Hilden Germany).

To minimize contaminations risks, batches were limited to 11 samples for run, alongside a reagent-only blank. Paraffin was removed by treating the sections with 1 mL of xylene, followed by vigorous vortexing (800 rpm) and incubation at 27°C for 10 minutes on a ThermoMixer[®] C (Eppendorf). Samples were then centrifugated at 14000 rpm for 5 minutes, and the supernatant was discarded.

The pellet was washed with 1 mL of absolute ethanol, vortexed briefly (15 seconds), incubated at room temperature for 5 minutes, centrifugated again at maximum speed for 2 minutes and air-dried at 37°C to eliminate residual solvent.

Subsequently, 180 μL of ATL buffer and 20 μL of proteinase K were added to each sample, followed by incubation at 56°C under agitation (650 rpm) until complete tissue lysis. A high-temperature incubation step at 90°C for 1 hour was included to partially reverse formalin-induced cross-linking. After brief centrifugation to collect condensate, samples were loaded onto the QIAcube instrument for automated extraction. The selected QIAcube protocol consists of four main steps: sample lysis, binding of nucleic acids to the silica membrane under high-salt conditions, sequential wash steps to remove contaminants while bound nucleic acids and final elution. Extracted nucleic acids were stored at -80°C until further analysis.

The concentration of the extracted DNA was assessed using a Qubit fluorometer (Thermo Fisher Scientific, Waltham, MA, USA). This method is based on the use of fluorescent dyes that emit signal only when specifically bound to the target molecule, enabling precise quantification of double-stranded DNA (dsDNA), single-stranded DNA (ssDNA) and RNA. The emitted fluorescence is directly proportional to the concentration of the target, allowing accurate quantification even at low concentrations, with high specificity and reproducibility.

A standard curve was first generated using two calibration standards of known concentration, provided with Qubit assay kit. Subsequently, the fluorescence readings of unknown samples were interpolated on this curve to calculate DNA concentrations.

The working solution was prepared by diluting the fluorescent reagent in the assay buffer at a 1:200 ratio, as per the manufacturer's protocol. This reaction mix was then aliquoted into dedicated assay tubes and combined with the standards and samples in appropriate volumes. Specifically, each standard reaction consisted of 190 μL of buffer and 10 μL of nucleic acid, while each sample reaction consisted of 190-199 μL of buffer and 1-10 μL of nucleic acid. After brief vortexing, the tubes were incubated at room temperature for 2-3 minutes to allow complete dye-target binding. Measurements were carried out by placing the standards first, followed by the

samples, into the fluorometer. Results were expressed in ng/ μ L and used to determine the suitability of each extract for downstream molecular analysis.

The presence of FcaPV infection was investigated through molecular detection of viral DNA in the extracted samples. Specifically, real-time PCR assays were employed to detect the presence of L1 gene fragments from various FcaPV types using distinct TaqMan[®] probes.

TaqMan probes allow accurate detection of specific DNA sequences based on fluorescence emission. Each probe is flanked by a fluorophore and a quencher: in the intact probe, the quencher suppresses fluorescence due to its proximity to the fluorophore. During amplification, if the target DNA is present and complementary to the probe, the Taq DNA polymerase, through its 5'-3' exonuclease activity, hydrolyses the bound probe. This enzymatic cleavage separates the fluorophore from the quencher, enabling fluorescence emission directly proportional to the amount of amplified product.

In this study, FAM-labelled probes (emission: 520-530 nm, yellow-green spectrum) with TAMRA quenchers were used. The reactions were performed using the iTaq[™] Universal Probes Supermix (Bio-Rad), prepared by combining the Supermix, RNase-free water, primers and probe in the proportions reported in Table 2.

Table 2 Reagents mix for qPCR using TaqMan probe (iTaq[™] Universal Probes Supermix)

Component	Volume
MM Biorad 2X	12.5 μ L
Primer F (20 μ M)	1.25 μ L
Primer R (20 μ M)	1.25 μ L
Probe 1:5	0.25 μ L
RNase-free H ₂ O	4.75 μ L

Table 3 Thermocycler settings for qPCR using TaqMan probe (iTaq[™] Universal Probes Supermix)

Cycling Step	Time	Temperature
Enzyme activation	5 minutes	95°C
Denaturation	15 seconds	95°C
Annealing/Extension	45 seconds	60°C

Aliquots of the master mix were dispensed into 96-well PCR plates and 5 μ L of extracted DNA from each sample was added to the corresponding wells. Plates were sealed with optical adhesive film to prevent evaporation, centrifugated at 3500 rpm for 5 minutes to eliminate air bubbles and loaded into a real-time thermal cycler under the conditions described in Table 3. Each run included technical replicates of each sample, to account for experimental variability, and a negative control (using RNase-free water), to monitor contamination.

Table 4 reports the sequences of primers and probes used for the detection of FcaPV.

Table 4 Primer sequences, probe sequences, annealing temperature, and amplicon length for the L1 genes of FcaPVs and the reference gene B2M.

GENE (Accession number)	PRIMERS	PROBE	Target	T (°C)	Bp
FcaPV1 L1 (NC_004765.1)	F: TCACCATACGGCTCATTTC R: AGGATGGTGACATGGTGGAT	TGCAGACACACAGTGCAAATACCC	DNA	58	145
FcaPV2 L1 (NC_038520)	F: TGACCACGCACACTTGAATA R: TACACGCGGTACCAATTCA	GCATCCCCTCAGGAATATGATGCCA	DNA	58	137
FcaPV3 L1 (NC_021472.1)	F: CTGCTGTGGAAGTGTGTAGG R: AAGATTGGTATGGCGTTTGC	TAGGCCGGGGAGGGCCTTTG	DNA	58	134
FcPV4 L1 (NC_022373.1)	F: CACTTGGGGTGCCAAAGTAGT R: GGGAAAGCGTGAGCAGTTGTA	GCTCCAAGGGCTGATGCCCC	DNA	60	148
FcPV5 L1 (NC_035479.1)	F: CAAAAACTCCGCCCCAGTG R: ACTGCAGTACCCCTAAGGA	GCGCCTTCCTCAGACCTGGA	DNA	60	120
FcPV6 L1 (MN857145)	F: GCTTGGGATCCACAGACACA R: AGGTATTCAGGTTGGGCGTG	GTGGGCCCTTGGGAGTGTCT	DNA	60	142
B2M (NM_001009876.1)		ACTCCCGTCACCCAGCAG	DNA	60	

7.5 RNA extraction, cDNA synthesis and viral oncogene expression analysis

Total RNA was extracted following a workflow analogous to that used for DNA, employing the Maxwell® RSC Viral Total Nucleic Acid Kit (Promega, Madison, WI, USA) in combination with the automated QIAcube® platform (Qiagen, Hilden, Germany), allowing simultaneous recovery of DNA and RNA from the same FFPE tissue samples. RNA quantification was performed using Qubit™

fluorometer (Thermo Fischer Scientific, Waltham, MA, USA). Extracted RNA was stored at -20°C until further processing.

Because PCR amplification is restricted to double-stranded nucleic acids, complementary DNA (cDNA) synthesis was required for downstream analyses. As total nucleic acids were co-extracted, an initial DNase digestion step was performed to eliminate residual genomic DNA, using the Reliance Select cDNA Synthesis Kit (Bio-Rad, Hercules, CA, USA). For each sample, 100 ng of RNA was used as template. DNase digestion was prepared by combining 0,5 µL of DNase with 1,5 µL of the appropriate reaction buffer, according to the manufacturer's instructions, before adding the mix to the RNA extract. 2 µL of this mix was added to 11 µL of RNA in 0,2 µL tubes. The mixture was gently homogenized to avoid enzyme inactivation and processed in a thermal cycler following the manufacturer's temperature profile (Table 5).

Table 5 Thermal cycler program for DNase treatment using the Reliance™ Select cDNA Synthesis Kit (Bio-Rad)

Cycling Step	Time	Temperature
DNA digestion	15 minutes	25°C
DNase inactivation	5 minutes	75°C

After DNA removal, reverse transcription was performed. The reaction was catalysed by reverse transcriptase, a DNA polymerase that uses RNA as template to synthesise complementary DNA (cDNA). The reaction mixture contained RNase-free water, engineered reverse transcriptase, 5x reaction buffer, deoxyribonucleotide triphosphates (dNTPs), and a combination of Oligo(dT) primers and random hexamer primers, annealing to multiple random sites along RNA molecules. This dual primer strategy was chosen to optimise performance: Oligo(dT) primers provide high specificity for mRNA but are less efficient with fragmented RNA, whereas random primers improve yield from degrade RNA but may also amplify non-mRNA targets.

In the reverse transcription step, primers annealed to complementary RNA sequences, allowing reverse transcriptase to synthesise the first cDNA strand, generating RNA-DNA hybrids. The RNA strand was subsequently degraded by RNase H activity or by reverse transcriptase itself, enabling synthesis of the second DNA strand.

For FFPE-derived RNA, the reaction mix (final volume 20 μ L) was prepared according to the manufacturer's recommendations (Table 6), gently vortexed and centrifugated, then incubated in a thermal cycler using the specified temperature program (Table 7). Parallel reactions were set up without reverse transcriptase (RT-controls) using a pooled RNA aliquot from the study samples, to monitor potential residual genomic DNA contaminations.

Table 6 Reagent mix for the Reliance™ Select cDNA Synthesis Kit (Bio-Rad)

Component	Volume
Buffer 5X	4 μ L
Reverse transcriptase	1 μ L
Oligo(dT) primers	1 μ L
Random primers	1 μ L

Table 7 Thermal cycler program for the Reliance™ Select cDNA Synthesis Kit (Bio-Rad)

Cycling Step	Time	Temperature
Priming and reverse transcription	20-90 minutes	50°C
RT inactivation	1 minute	95°C

The resulting cDNA was diluted 1:5 in RNase-free water and stored at -20°C until quantitative PCR (qPCR) analysis of viral oncogene expression.

Quantitative PCR (qPCR) was applied to confirm the presence of FcaPV infection by detecting transcripts of the E6 and E7 viral oncogenes. Reactions were performed using the SsoFast™ EvaGreen® Supermix (Bio-Rad, Hercules, CA, USA), prepared by combining the reaction buffer and specific primers in the shown in Table 8. For each reaction, 2 μ L of cDNA (for RNA-derived assay) or 5 μ L (for DNA-based assays) were added to the reaction mix, and aliquots were dispensed into 96-well PCR plates. Plates were sealed with optical adhesive film, centrifugate to eliminate air bubbles and placed in a real-time thermal cycler under the condition detailed in Table 9.

Table 8 Reagents for qPCR using fluorescent dye chemistry (SsoFast EvaGreen, Bio-Rad)

Component	Volume
Buffer 5X	10 μ L
Primer F (2 μ M)	2 μ L
Primer R (2 μ M)	2 μ L
H ₂ O	4 μ L

Table 9 Thermal cycler settings for qPCR using fluorescent dye chemistry (SsoFast EvaGreen, Bio-Rad)

Cycling Step	Time	Temperature
Enzyme activation	30 seconds	95°C
Denaturation	5 seconds	95°C
Annealing/extension	5 seconds	55-60°C
Melt Curve	5 seconds	65-95°C

To monitor for possible environmental contaminations, each run included a no-template control (NTC) containing RNase-free water. All reactions were performed in duplicate.

The primer sequences used for amplification are reported in Table 10.

Table 10 Primer sequences, annealing and melting temperatures, and expected amplicon length for amplification of FcaPV E6 and E7 genes.

GENE (Accession number)	PRIMERS	Target	Ta (°C)	Tm (°C)	Bp
FcaPV1 E6 (NC_004765.1)	F: TGCCCAATCATCCTTCCACC R: ATCCAGTGCTGCCTCGAAA	cDNA	60	79,5	96
FcaPV2 E6 (NC_038520)	F: TCGGTCCGGGACATAAGTG R: AATATGGAGCGTCCTCGCA	cDNA	60	81	112
FcaPV3 E6 (NC_021472.1)	F: CGCCACACACCTCTGACTAA R: TTGTGCTTTGCCAGTTCGG	cDNA	60	82	112
FcPV4 E6 (NC_022373.1)	F: ACAATCGGCAACACCCTCTC R: AAAACTTGGTGGTGC GG TG	cDNA	60	20,5	127
FcPV5 E6 (NC_035479.1)	F: CGCACTAGATGCAAAGGCT R: GGGTGCTGTCTCCGTTTAT	cDNA	60	60	196
FcPV6 E6 (MN857145)	F: CCCAGAAGTTGCTGTTCT R: TCCAGATGGCAAAGGCGAA	cDNA	60	78,5	174
FcaPV1 E7	F: AGCTTCAACCAACACCCAAT R: CATCTCGCATCTCCGAAGTC	cDNA	60	-	139
FcaPV2 E7	F: GCCGCAGACGAGACTTAAA R: ACGTACCCTGTGGAGTGTG	cDNA	60	83	115
FcaPV3 E7	F: TTATCGCGATCCGCCATGTT R: AGTGCCACAAGCAGTCAGA	cDNA	60	83,5	112
FcPV4 E7	F: TATCCCCAGACCTGCCAAGA R: GAAGAGGAGGAGCCTGAG	cDNA	60	83,5	143
FcPV5 E7	F: AGACGTGGCAAAAACCCAG R: TTGCCCGCCAATTTACTTGC	cDNA	60	83	139
FcPV6 E7	F: AGATTCCGGACACAGCAGGA R: AGATTCCGGACACAGCAGGA	cDNA	60	-	85

8 – RESULTS

8.1 Immunohistochemical evidence of EMT

Immunohistochemical analysis was performed on all 50 cases of feline nasal planum squamous cell carcinoma using a panel of epithelial, mesenchymal, EMT-related and hypoxia-associated markers. The semi-quantitative immunoreactivity scoring ranged from 0 (no immunolabeled cells) to 4 (76-100% of immunolabeled cells), considering the percentage of positive tumor cells. Subcellular localization (cytoplasmic, membranous or nuclear) was also recorded when appropriate. The results are reported in Table 11.

Table 11 Summary of IHC Staining Patterns in Feline npSCC Cases - Semi-quantitative evaluation (0 = no staining; 1 = 1–25%; 2 = 26–50%; 3 = 51–75%; 4 = 76–100%.) of marker expression, detailing phenotype shifts associated with EMT and hypoxia in feline nasal planum SCC.

SLIDE N.	VIM	CK	E-CAD	N-CAD	β-CAT	HIF-1α overall	HIF-1α CIT	HIF-1α NUC	ZEB1 overall	ZEB1 CIT	ZEB1 NUC	TWIST-1 overall	TWIST-1 CIT	TWIST-1 NUC
1	2	2	3	1	2	0	0	0	0	0	0	0	0	0
2	1	3	3	0	3	2	2	1	0	0	0	0	0	0
3	0	2	2	0	3	1	0	1	0	0	0	2	0	2
4	0	2	3	1	3	1	0	1	0	0	0	0	0	0
5	1	3	2	0	3	1	1	0	0	0	0	1	1	0
6	1	3	3	0	3	2	2	0	0	0	0	0	0	0
7	1	2	2	0	3	1	1	0	0	0	0	0	0	0
8	1	3	2	1	3	1	0	1	0	0	0	2	2	0
9	2	2	2	0	3	0	0	0	0	0	0	0	0	0
10	0	2	3	0	2	0	0	0	0	0	0	0	0	0
11	1	2	3	0	3	0	0	0	0	0	0	0	0	0
12	1	2	2	0	3	0	0	0	0	0	0	0	0	0
13	0	2	3	1	2	2	1	1	0	0	0	0	0	0
14	2	2	2	0	3	1	0	1	0	0	0	1	1	0
15	1	2	2	0	3	0	0	0	0	0	0	0	0	0
16	1	3	3	0	3	2	0	2	0	0	0	2	0	2
17	1	2	2	1	2	1	1	0	0	0	0	1	1	0
18	1	2	3	0	3	1	1	0	0	0	0	0	0	0
19	2	2	3	0	3	0	0	0	0	0	0	0	0	0
20	2	2	2	0	3	1	0	1	0	0	0	0	0	0
21	1	2	2	0	3	0	0	0	0	0	0	0	0	0
22	0	2	3	0	3	3	3	0	2	1	1	1	0	1
23	1	2	3	0	3	0	0	0	1	1	0	0	0	0
24	1	2	2	0	3	1	1	0	1	1	0	0	0	0
25	2	2	2	0	3	0	0	0	0	0	0	1	1	0
26	1	2	2	0	2	0	0	0	1	0	1	0	0	0
27	1	3	3	0	3	0	0	0	0	0	0	0	0	0

28	1	2	3	0	3	1	1	0	0	0	0	0	0	0
29	1	2	3	0	4	0	0	0	0	0	0	2	0	2
30	0	3	2	0	3	0	0	0	0	0	0	0	0	0
31	1	2	3	0	3	0	0	0	2	1	1	0	0	0
32	2	3	2	0	3	1	1	0	1	1	0	1	1	0
33	1	3	2	0	3	2	1	2	1	0	1	0	0	0
34	1	3	3	0	3	0	0	0	0	0	0	0	0	0
35	2	3	1	0	4	0	0	0	1	1	0	0	0	0
36	1	2	4	0	3	1	1	0	0	0	0	0	0	0
37	0	2	2	0	3	2	0	2	0	0	0	0	0	0
38	0	3	3	0	3	0	0	0	0	0	0	0	0	0
39	2	2	2	0	3	0	0	0	0	0	0	0	0	0
40	1	3	4	0	3	0	0	0	0	0	0	0	0	0
41	2	2	2	0	3	2	0	2	0	0	0	0	0	0
42	1	2	2	1	3	2	1	1	0	0	0	0	0	0
43	1	2	2	1	3	1	1	0	0	0	0	0	0	0
44	1	2	2	0	4	1	0	1	0	0	0	1	1	0
45	1	3	3	0	3	1	1	0	0	0	0	0	0	0
46	0	2	3	0	3	2	2	0	0	0	0	0	0	0
47	1	3	3	0	3	0	0	0	0	0	0	0	0	0
48	0	3	3	0	3	1	0	1	0	0	0	0	0	0
49	0	2	3	0	3	0	0	0	0	0	0	0	0	0
50	2	3	3	0	3	0	0	0	0	0	0	0	0	0

Pan-cytokeratin (AE1/AE3) was expressed in all cases, with moderate to strong labelling (score 2-4) in the neoplastic epithelial component, confirming epithelial origin (Fig. 3A). Vimentin immunoreactivity was detected in 78% (39/50) of tumors, with a maximum score of 2. Expression was often stronger at the invasive front and distribution was predominantly cytoplasmic in tumor cells (Fig. 3D).

E-cadherin expression was preserved (score 3-4) in 52% (26/50) of cases, while partial or complete loss (score 0-2) was observed in 48% (24/50) (Fig. 3B). N-cadherin was absent in 86% (43/50) of tumors (score 0), while 14% (7/50) displayed focal positivity (score 1), for this reason is not possible, in this case, to talk about “cadherin switch” (Fig. 3C).

β -catenin was detected in all tumors, predominantly with strong membranous labelling (90%, score 3-4). Aberrant cytoplasmic and/or nuclear localization was rare, observed in < 10% of cases and was generally focal.

HIF-1 α expression was observed in 54% (27/50) of cases, mostly with low to moderate scores (1-2), only one case showed a score of 3. Cytoplasmic staining was more frequent (34%, 17/50) than nuclear positivity (28%, 14/50). Cases with nuclear HIF-1 α tended to show concurrent cytoplasmic labelling.

ZEB1 expression was detected in 16% (8/50) of tumors, with both cytoplasmic and nuclear labelling patterns. Nuclear ZEB1 positivity was found in 8% (4/50) of cases, cytoplasmic staining was more frequent (12%, 6/50) mostly focal (score 1) (Fig. F). TWIST-1 was positive in 22% (11/50) of tumor, with cytoplasmic staining in 14% (7/50) and nuclear staining in 8% (4/50). Nuclear labelling was generally low intensity and focal, often at the invasive tumor front (Fig. E).

Table 12 Immunohistochemical scores (0–4) of control feline nasal planum tissues for the tested markers (CK, E-cadherin, N-cadherin, vimentin, β -catenin, HIF-1 α , TWIST-1, ZEB1).

SLIDE N.	VIM	CK	E-CAD	N-CAD	β -CAT	HIF-1 α	ZEB1	TWIST-1
1C	1	4	4	0	3	1	0	0
2C	0	4	4	1	4	0	0	0
3C	0	4	3	0	4	0	0	0
4C	0	3	4	0	3	1	0	0
5C	0	4	4	0	4	0	0	1
6C	0	4	4	0	4	0	0	0
7C	1	3	4	0	3	0	0	0
8C	0	3	3	0	4	0	0	0
9C	0	4	4	0	4	0	1	0
10C	0	4	4	0	4	0	0	0

In normal feline nasal planum tissues (Table 12) pan-cytokeratin and E-cadherin show strong, diffuse epithelial staining (score 3-4) with membranous localization. β -catenin is predominately membranous (score 3-4). Mesenchymal markers and EMT-related transcription factors were almost entirely absent, although a few cases displayed focal weak positivity (score 1). Such findings are considered within the physiological range. The control samples displayed the expected epithelial immunophenotype, confirming their suitability as a reference for comparison with neoplastic tissues.

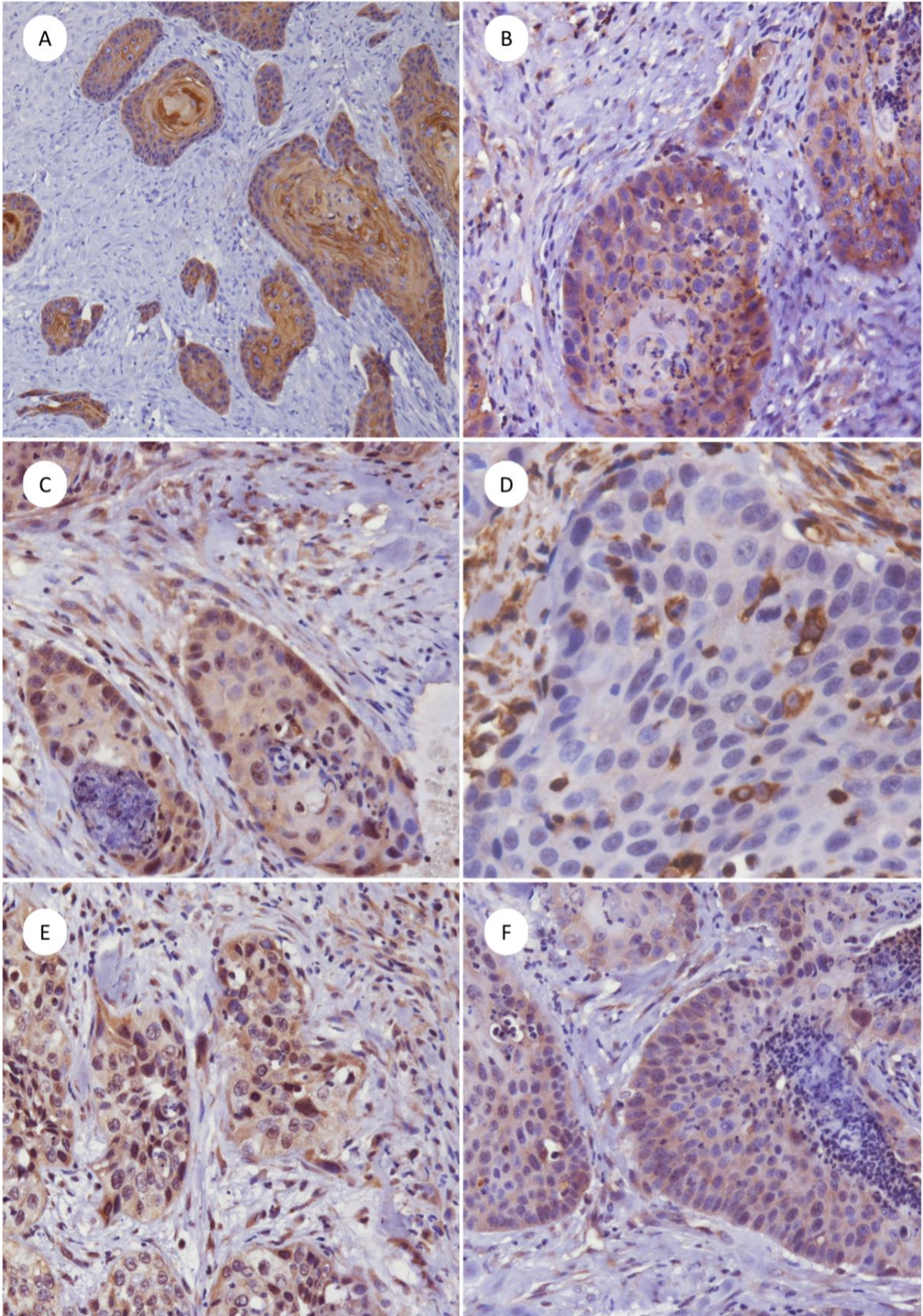


Figure 3. Immunohistochemical staining of the same feline nasal planum SCC case. A – pan-cytokeratin 10X, B – E-cadherin 20X, C – N-cadherin 20X, D – vimentin 40X, E – TWIST-1 20X, F – ZEB1 20X.

8.2 FcaPV molecular detection

Detection of L1 was carried out using a TaqMan®-based qPCR assay, which ensured high target specificity, real-time quantification and minimized the risk of non-specific amplification. Alongside each L1 test, amplification of B2M reference gene was performed as an internal control to assess nucleic acid integrity. As B2M amplification was successful in all tested samples, the validity of the analyses was confirmed, and all L1-negative results were considered true negative. Results are reported in Table 13.

FcaPV DNA was detected in 32 out of 50 npSCC cases (64%), with single or multiple genotype infections. Among the positive samples, the most prevalent type was FcaPV2, identified in 25 cases (78%), either alone or in combination with other types. FcaPV3 was detected in 12 cases (37%), while FcPV4 was found in 7 cases (21%). FcaPV1, FcaPV5 and FcaPV6 were not detected in any sample.

Co-infections with two FcaPV type were observed in 12/32 cases (37%). The most frequent co-infection patterns were FcaPV-2 + FcaPV3 (n=7) and FcaPV-2 + FcaPV-4 (n=5).

Among the 10 negative control samples obtained at necroscopy 1/10 (10%) tested positive for FcaPV-2, while the remaining nine controls were negative for all screened genotypes. The presence of FcaPV DNA in that single control may reflect subclinical carriage or low-level viral persistence in clinically normal tissue.

Table 13 Type-specific detection of Felis catus papillomavirus (FcaPV) DNA by TaqMan real-time PCR in 50 feline nasal planum SCCs. Presence (+) or absence (-) of each FcaPV genotype is indicated.

SLIDE NUMBER	FcaPV1	FcaPV2	FcaPV3	FcaPV4	FcaPV5	FcaPV6
1	-	+	-	+	-	-
2	-	+	+	-	-	-
3	-	+	-	-	-	-
4	-	-	-	-	-	-
5	-	-	-	-	-	-
6	-	-	-	-	-	-
7	-	+	-	-	-	-
8	-	-	-	-	-	-

9	-	+	+	-	-	-
10	-	-	-	-	-	-
11	-	+	+	-	-	-
12	-	+	-	-	-	-
13	-	+	-	-	-	-
14	-	+	-	-	-	-
15	-	+	-	+	-	-
16	-	+	-	-	-	-
17	-	+	+	-	-	-
18	-	+	+	-	-	-
19	-	+	-	-	-	-
20	-	-	-	-	-	-
21	-	+	-	-	-	-
22	-	+	-	+	-	-
23	-	-	+	-	-	-
24	-	+	-	+	-	-
25	-	-	-	+	-	-
26	-	-	-	-	-	-
27	-	-	+	-	-	-
28	-	-	-	-	-	-
29	-	-	-	-	-	-
30	-	+	-	-	-	-
31	-	+	-	-	-	-
32	-	-	+	-	-	-
33	-	-	-	-	-	-
34	-	+	+	-	-	-
35	-	-	-	-	-	-
36	-	-	-	-	-	-
37	-	+	-	-	-	-
38	-	-	-	+	-	-
39	-	-	-	-	-	-
40	-	-	+	-	-	-
41	-	-	-	-	-	-
42	-	-	-	-	-	-
43	-	+	-	-	-	-
44	-	-	-	-	-	-
45	-	+	+	-	-	-

46	-	+	-	+	-	-
47	-	-	-	-	-	-
48	-	+	-	-	-	-
49	-	-	-	-	-	-
50	-	-	+	-	-	-

8.3 Evaluation of oncogene expression

In this study, the expression of E6 and E7 was evaluated by qPCR in all samples that tested positive for L1 DNA. Amplification was performed using SYBR Green dye, which enabled real-time quantification of the target. In parallel, the B2M reference gene was amplified in each sample to confirm RNA integrity and normalize oncogene expression level. All samples expressed B2M, confirming the overall quality of nucleic acids.

E6/E7 transcript were detected in all L1-positive samples except one (case n. 25). This suggests that in this case, the FcaPV infection may not have been causally involved in the neoplastic process. The specificity of each positive result was confirmed by comparing the observed melting temperature with the theoretical T_m , calculated based on primer sequence composition using the formula: $T_m = 2^{\circ}C * (A + T) + 4^{\circ}C * (G + C)$

Overall, 95% of L1-positive npSCC also expressed E6/E7, strongly supporting the presence of an active, transcriptionally engaged viral infection in most FcaPV-associated cases.

8.4 Correlation between FcaPV status and immunohistochemical findings

To explore the potential association between papillomavirus infection status and EMT-related changes, immunohistochemical scores were compared between FcaPV-positive npSCC, FcaPV-negative npSCC and control tissues. Representative violin plots illustrating the distribution of HIC scores across groups are shown in Figures 4-7, generated using RStudio software.

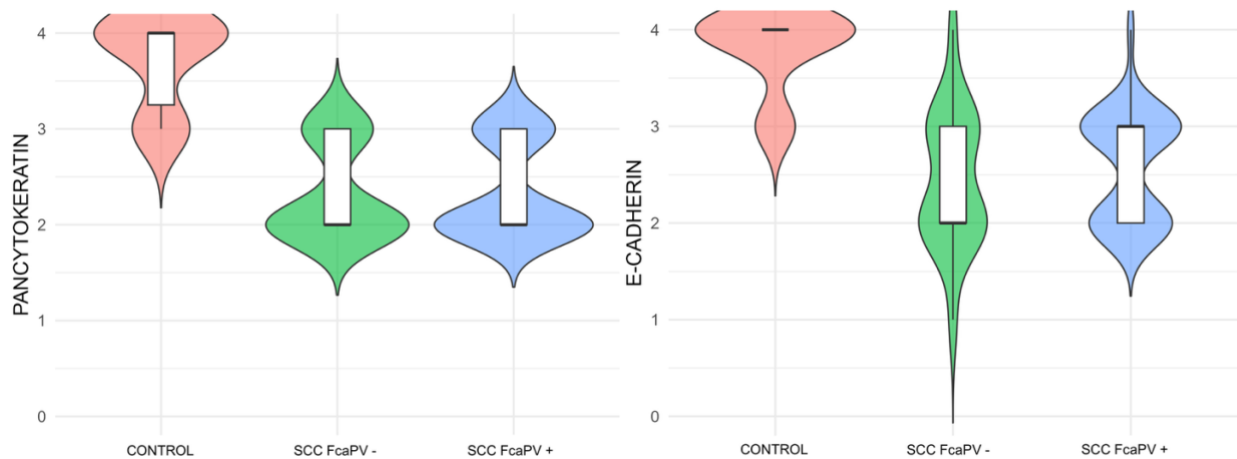


Figure 4. Pan-cytokeratin and E-cadherin expression across groups. Violin plot of semi-quantitative AE1/AE3 cytokeratin and E-cadherin IHC score (0-4) in feline nasal planum SCC stratified by FcaPV status (FcaPV-positive: blue / FcaPV-negative: green) and normal control tissue (red).

Pan-cytokeratin (Fig. 4) expression was consistently high in control tissue, with scores concentrated at 4, reflecting preserved epithelial phenotype. In contrast, both FcaPV-positive and negative tumors showed reduced expression (median score = 2), but without significant differences between the two groups.

E-cadherin (Fig. 4) expression showed partial loss in both tumor groups. Median scores tended to be lower in PV-negative tumors compared with PV-positive ones, indicating greater impairment of cell-cell adhesion. As expected, control tissues showed strong membranous expression, with scores clustered at the maximum value (median score = 4).

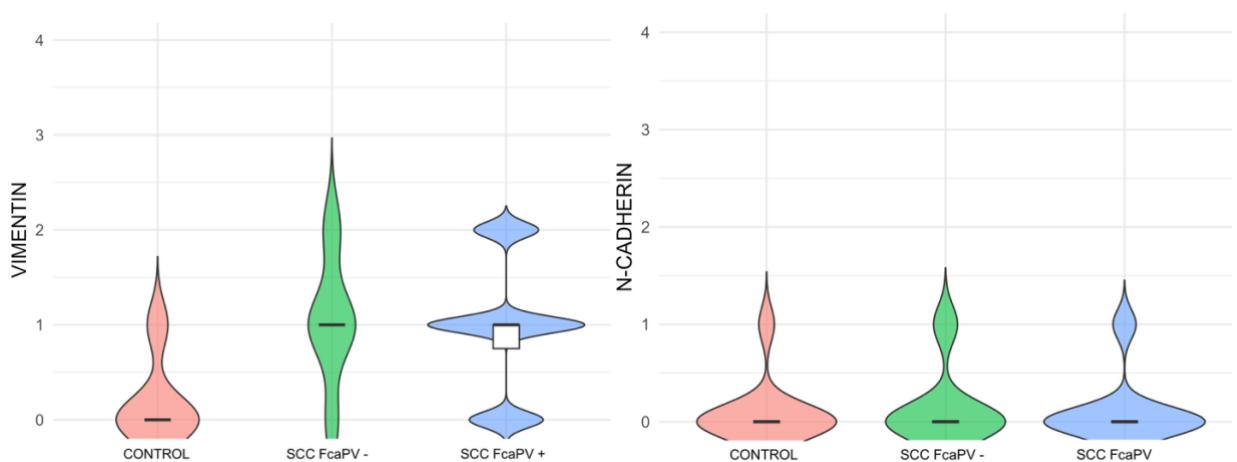


Figure 5. Vimentin and N-cadherin expression across groups. Violin plot of semi-quantitative vimentin and N-cadherin IHC score (0-4) in feline nasal planum SCC stratified by FcaPV status (FcaPV-positive: blue / FcaPV-negative: green) and normal control tissue (red).

Vimentin (Fig. 5) expression was consistently absent in control tissue (median score = 0), but detected in both PV-positive and PV-negative npSCC with a trend toward higher scores in PV-negative tumors (median score = 1).

N-cadherin (Fig. 5) expression was rare overall, with only focal positivity in a minority of cases, and no significant differences across groups (median score = 0).

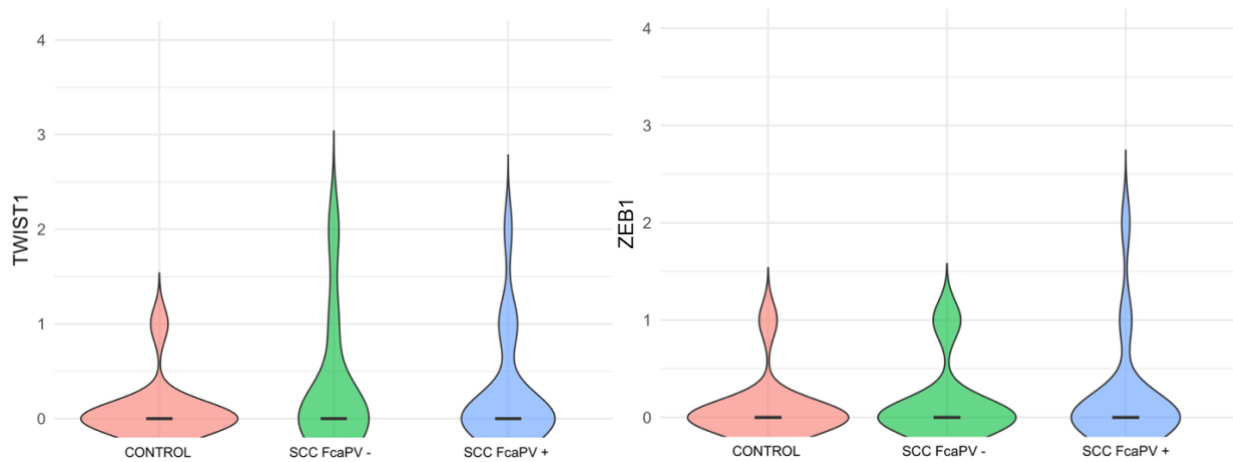


Figure 6. TWIST-1 and ZEB1 expression across groups. Violin plot of semi-quantitative TWIST-1 and ZEB1 IHC score (0-4) in feline nasal planum SCC stratified by FcaPV status (FcaPV-positive: blue / FcaPV-negative: green) and normal control tissue (red).

Nuclear expression of TWIST-1 and ZEB1 (Fig. 6) was infrequent but restricted to tumor groups. ZEB1 was slightly more frequent in PV-positive tumors, TWIST-1 positivity was more often observed in PV-negative tumors. All controls were negative.

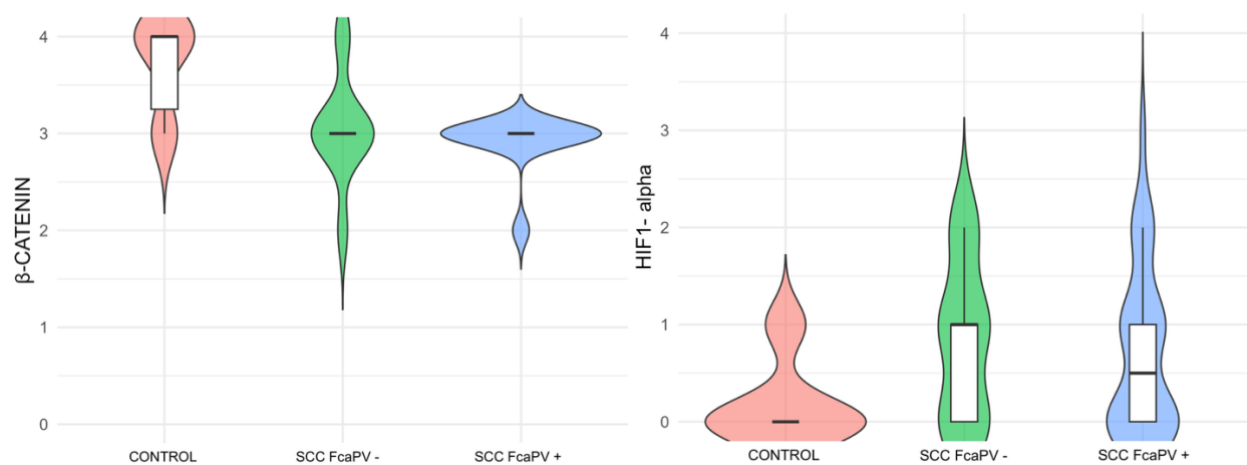


Figure 7. β -catenin and HIF-1 α expression across groups. Violin plot of semi-quantitative β -catenin and HIF-1 α IHC score (0-4) in feline nasal planum SCC stratified by FcaPV status (FcaPV-positive: blue / FcaPV-negative: green) and normal control tissue (red).

In control tissues, β -catenin (Fig. 7) showed consistently strong membranous expression (median score = 4), reflecting normal epithelial architecture. In contrast, both FcaPV-positive and negative npSCC exhibited reduced expression compared to controls. FcaPV-negative tumors displayed a wider variability, FcaPV-positive tumors showed a more uniform expression pattern, but the median score was the same (median score = 3).

HIF-1 α (Fig. 7) expression was observed in both tumor groups, with PV-positive tumors showing higher overall scores compared to PV-negative ones. Controls showed only minimal or absent staining (median score = 0).

9 – DISCUSSION

Feline nasal planum squamous cell carcinoma (npSCC) represents a biologically and clinically relevant neoplasm in feline oncology, characterized by locally aggressive behaviour and a multifactorial pathogenesis. Historically, chronic ultraviolet (UV) exposure has been regarded as a primary etiological driver of cutaneous SCC in cats, particularly in lightly pigmented and sparsely haired regions. However, over the last decade, accumulating evidence has supported a contributory role of *Felis catus* papillomaviruses (FcaPV) in feline SCC arising in UV-protected sites, where viral DNA and, crucially, transcriptional activity of viral oncogenes have been demonstrated. Within this framework, npSCC represents a model to explore virus-associated oncogenesis and the potential interaction with epithelial-mesenchymal transition (EMT), a key biological program underlying tumor invasion, cellular plasticity and therapeutic resistance.

In the present study, FcaPV DNA was detected in 64% of npSCC cases, with FcaPV-2 being the most prevalent genotype. This prevalence is coherent with previous studies reporting a strong association between FcaPV and cutaneous or mucosal SCC in cats (40,102,119). The identification of multiple viral genotypes in 12 tumors further supports the concept that chronically damaged epithelia may host complex viral communities. Although the biological significance of co-infection remains incompletely understood, this finding may reflect either true viral coexistence within a permissive tumor microenvironment or long-term persistence of multiple viral types within a field of chronically altered epithelium. Similar scenarios have been described in HPV-associated tumorigenesis in humans, where multiple viral genotypes may be detected within dysplastic or neoplastic epithelia (49,120).

A major strength of the present study lies in the integration of viral oncogene expression analyses to support biological relevance. From a pathogenic point of view, detection of viral DNA alone is insufficient to establish a causal relationship between papillomavirus infection and tumorigenesis. The L1 gene, although highly conserved and widely used for screening purposes, primarily reflects viral presence and does not provide information on viral integration or oncogenic activity. Integration events may occur with partial or complete loss of the L1 region while retaining expression of E6 and E7 oncogenes, potentially leading to false-negative results if DNA-based assays are used in isolation. Conversely, detection of L1 DNA in the absence of oncogene

transcription may reflect latent or incidental viral carriage rather than biologically meaningful infection.

For these reasons, the transcriptional activity of viral oncogenes represents a critical step to demonstrate causality. In this study, the expression of E6/E7 oncogenes was confirmed in most L1-positive cases (95%), supporting the notion that viral infection is not incidental, but biologically active in tumor tissue. This observation is crucial, since transcriptional activity of papillomaviruses has been widely recognized as the discriminating factors between “passenger” versus “driver” infections (54,117,121). The oncogenic functions of FcaPV closely mirror those of high-risk HPV, particularly through the conserved activities of E6 and E7 oncoproteins. E6 promotes p53 degradation, while E7 inactivates pRb, driving uncontrolled proliferation and resistance to apoptosis, mechanisms consistently described in both human and veterinary oncology (44,47,100,102).

The present study also confirmed the immunohistochemical evidence of EMT in feline nasal planum SCC, as demonstrated by the frequent loss or reduction of E-cadherin, acquisition of vimentin, and focal nuclear expression of EMT-associated transcription factors such as TWIST-1 and ZEB1. These findings reinforce the notion that EMT represents a relevant biological process in feline SCC, consistent with previous veterinary reports (13,49) and with evidence from human oncology, where HPV-positive cervical and oropharyngeal SCC display down-regulation of epithelial markers, up-regulation of mesenchymal markers and nuclear over-expression of TWIST-1, Snail and ZEB1 (61,62,114,115).

When directly comparing FcaPV-positive and FcaPV-negative tumors, no statistically significant differences were observed in the expression patterns of EMT-related markers. Nevertheless, correlation analyses revealed subtle but consistent trends: FcaPV-positive tumors displayed relatively higher ZEB1 and HIF-1 α expression, whereas FcaPV-negative tumors were more frequently associated with E-cadherin loss and vimentin overexpression. These patterns may reflect distinct pathogenetic trajectories. The presence of EMT features in both groups reinforces the notion that EMT is a common endpoint in SCC progression, but viral and non-viral tumors may achieve it through partially divergent mechanism.

Comparable findings have been reported in human oropharyngeal SCC, where Lefevre et al. (122) showed that EMT features were not significantly associated with HPV status. The authors suggested that EMT in these tumors may arise from the convergence of viral and non-viral carcinogenic drivers, ultimately activating shared downstream pathways rather than reflecting a virus-specific biological program. This concept challenges a simplistic causal link between viral infection and EMT activation and instead supports a multifactorial and context-dependent model.

In line with this interpretation, Barillari et al. (120) proposed a conceptual framework in which high-risk HPV infection and EMT represent interconnected but not obligatorily simultaneous events during squamous tumorigenesis of the uterine cervix. According to this model, viral oncogene expression may initiate molecular alterations that predispose epithelial cells to EMT, while additional host-related and microenvironmental factors, such as inflammation, hypoxia and stromal interactions, are required for full EMT activation.

Within the framework of comparative oncology, evidence of EMT has also been reported in equine genital squamous cell carcinoma associated with EcPV-2 infection. Interestingly, in these tumors EMT appears to be predominantly driven by cadherin switching, with loss of E-cadherin and up-regulation of N-cadherin, and by activation of hypoxia-related and Wnt/ β -catenin pathways. In particular, nuclear accumulation of β -catenin and up-regulation of HIF-1 α have been consistently reported in EcPV-2 positive penile and vulval SCC (16,55,56). These findings suggest that, in horses, papillomavirus-driven carcinogenesis engages EMT through a different mechanism compared with feline npSCC, where intermediate filament re-arrangements and focal activation of transcription factors such as TWIST-1 and ZEB1 are more prominent.

Further insight is provided by studies addressing tumor cell plasticity in equine head and neck SCC. Strohmayer et al. (123) demonstrated that both EcPV-positive and EcPV-negative tumors exhibit pronounced cellular plasticity and partial EMT phenotypes irrespective of viral status. EMT-related alterations, including changes in cytokeratin expression, vimentin up-regulation and activation of EMT-associated transcription factors, were detected across both groups, with marked intra-tumoral heterogeneity.

Support for this interpretation also comes from recent high-resolution studies in human HPV-associated head and neck SCC. Using single-cell RNA sequencing, Bedard et al. (124) demonstrated that HPV-positive and HPV-negative tumors share substantial intra-tumoral epithelial heterogeneity, with multiple malignant cell subpopulations spanning a continuum of differentiation states and EMT-related transcriptional programs. Notably, EMT-associated gene expression was neither uniform across tumors nor restricted to HPV-positive cases, but instead confined to specific cellular subsets shaped by local microenvironmental cues.

Finally, the dynamic and reversible nature of EMT has been further highlighted by studies examining circulating tumor cells (CTC) in HPV-associated head and neck SCC. Ida et al. (125) showed that EMT-related gene expression differs markedly between primary tumors and CTC, and that HPV-positive tumors do not necessarily display a uniform EMT signature at the tissue level. Interestingly, EMT-associated transcription factors such as TWIST-1 and ZEB1 were down-regulated in HPV-positive primary tumors but up-regulated in CTC, underscoring the influence of tumor microenvironment, immune interactions and metastatic dissemination on EMT programs.

In veterinary medicine, this conceptual framework has been further reinforced by a recent comprehensive review by Tutu et al. (118), which summarizes current advances in feline oral squamous cell carcinoma and outline future perspectives in the study of PV-associated feline tumors. The authors emphasize that, similarly to human HPV-driven SCC, feline SCC represents a complex and heterogeneous disease in which viral infection, host epithelial susceptibility, tumor microenvironment and cellular plasticity collectively shape tumor behaviour. In particular, Tutu et al. (118) highlight EMT as a key biological process involved in invasion, progression and therapeutic resistance in feline SCC, while underscoring that EMT activation cannot be attributed solely to viral infection. These considerations closely align with the findings of the present study, in which EMT-related immunohistochemical alterations were frequently observed in feline nasal planum SCC irrespective of FcaPV status, supporting the notion that EMT represents a shared biological endpoint in SCC progression rather than a virus-specific hallmark.

This study presents several limitations that should be acknowledged. First, the retrospective design and the use of FFPE samples may have impacted nucleic acid integrity and limited the sensitivity of molecular analyses. Second, validation of EMT activation was restricted to

immunohistochemical evaluation, without complementary in vitro assays to confirm the direct role of viral oncogenes in modulating EMT-related pathways. Third, the sample size may still be insufficient to detect subtle differences in immunohistochemical or molecular patterns between FcaPV-positive and FcaPV-negative tumors. This limitation is particularly relevant when evaluating complex biological processes such as EMT, which is recognized as a dynamic and heterogeneous spectrum rather than a binary event. Subtle shift in EMT-related marker expression, partial EMT phenotypes or differences confined to specific tumor subregions (e.g. invasive front versus tumor core) may therefore not reach statistical significance in cohort-based analyses.

An additional limitation of the present study is that only a subset of viral types was investigated in the molecular analyses. Consequently, a proportion of tumors classified as FcaPV-negative may theoretically harbour other, less common or recently described genotypes that were not included in the screening panel, potentially influencing the proportion of negative cases and partially affecting the comparative analyses between FcaPV-positive and FcaPV-negative tumors. However, the selection of FcaPV genotypes included in this study was based on the state of knowledge at the time of study design, focusing on the best-characterized viral types with documented or suspected oncogenic potential, particularly FcaPV-2 and FcaPV-4. Other genotypes were either rarely reported, lacked evidence of transcriptional activity or oncogenic involvement, or were described only after the completion of the experimental phase, such as the recently identified FcaPV-11. From a methodological perspective, validated and FFPE-optimized assays were available only for the selected genotypes, ensuring analytical reliability.

Finally, clinical outcome data such as recurrence, metastatic progression, disease-free interval or overall survival were not available, precluding correlation of FcaPV status and EMT-related features with prognosis. In addition, the lack of correlation between viral infection status or EMT activation and tumor-related parameters, including histological grade or the presence and intensity of inflammatory infiltrates represents a further limitation. Inflammation itself is a well-recognized independent inducer of EMT and may therefore act as a confounding factor, partially obscuring the specific contribution of viral infection to EMT-related changes in feline nasal planum SCC.

Future studies are warranted to further elucidate the complex interplay between FcaPV infection and EMT in feline nasal planum SCC. Prospective investigations integrating larger, multicentric

cohorts would be essential to increase statistical power and to better capture the biological heterogeneity of EMT-related phenotypes. In this context, the inclusion of detailed clinicopathological data, such as histological grade, inflammatory infiltrate, recurrence, metastatic behaviour and survival outcomes, would allow a more robust assessment of the prognostic significance of both viral status and EMT activation. Complementary functional approaches are needed to validate the causal role of viral oncogenes in EMT modulation. In vitro models based on feline SCC-derived cell lines or ex vivo tissue systems could be employed to directly investigate the effect of FcaPV E6 and E7 expression on EMT-related signalling pathways. Further molecular studies should also aim to expand the spectrum of investigated FcaPV genotypes, incorporating recently identified viral types, this would allow a more comprehensive evaluation of viral diversity and its potential contribution to tumor biology. Finally, comparative and translational studies integrating feline, equine and human PV-associated SCC may provide valuable insights into conserved and species-specific mechanisms of viral-driven tumor plasticity.

In this One Health perspective, feline nasal planum SCC may represent a particularly informative spontaneous model to study the interaction between viral oncogenesis, EMT and the tumor microenvironment, with potential implications for both veterinary and human oncology.

10 – CONCLUSION

Feline nasal planum squamous cell carcinoma represents a clinically relevant neoplasm and a relevant spontaneous model for studying papillomavirus-associated carcinogenesis in veterinary and comparative oncology. In this study, FcaPV DNA was detected in a large portion of npSCC cases, with FcaPV-2 as the most prevalent genotype. Importantly, transcriptional activity of viral oncogenes E6 and E7 was demonstrated in the majority of L1-positive tumors, supporting the role of FcaPV as a biologically active factor rather than an incidental finding in feline cutaneous tumorigenesis.

Immunohistochemical analyses confirmed the presence of EMT features in npSCC, including down-regulation of epithelial markers, up-regulation of vimentin and focal nuclear expression of EMT-related transcription factors. However, no statistically significant differences in EMT marker expression were observed between FcaPV-positive and FcaPV-negative tumors. These findings indicate that EMT represents a common biological endpoint in SCC progression, independent of viral status, suggesting that both viral and non-viral tumors converge toward similar phenotypic programs through distinct mechanisms.

Comparative evaluation across species highlighted both shared and divergent aspects of PV-driven tumorigenesis. While human HPV-associated SCC and equine EcPV-related SCC frequently exhibit EMT characterized by cadherin switching and activation of hypoxia and Wnt/ β -catenin pathways, feline npSCC appears to rely more prominently on intermediate filament reorganization and focal activation of key EMT transcription factors.

Overall, this study provides an integrated molecular and immunohistochemical characterization of feline nasal planum SCC, combining viral genotyping, oncogene expression analysis and EMT profiling. Within a One Health and comparative oncology framework, feline npSCC emerges as a useful model to explore conserved and divergent mechanisms of PV-associated tumorigenesis. Future studies incorporating a broader spectrum of viral genotypes, functional approaches and clinical outcome data will be essential to further define the prognostic and therapeutic relevance of viral infection and EMT activation in feline SCC.

BIBLIOGRAFIA

1. Goldschmidt MH, Goldschmidt KH. Epithelial and melanocytic tumors of the skin. In: Tumors in Domestic Animals. 5th edn Wiley-Blackwell; 2017. p. 88–141.
2. Murphy S. Cutaneous squamous cell carcinoma in the cat: current understanding and treatment approaches. J Feline Med Surg. 2013 May;15(5):401–7.
3. Munday JS, Gwyther S, Thomson NA, Malik R. Bilateral pre-auricular papillary squamous cell carcinomas associated with papillomavirus infection in a domestic cat. Vet Dermatol. 2017 Apr;28(2):232.
4. Sequeira I, Pires MDA, Leitão J, Henriques J, Viegas C, Requicha J. Feline Oral Squamous Cell Carcinoma: A Critical Review of Etiologic Factors. Vet Sci. 2022 Oct 11;9(10):558.
5. Gasymova E, Meier V, Guscetti F, Cancedda S, Roos M, Rohrer Bley C. Retrospective clinical study on outcome in cats with nasal planum squamous cell carcinoma treated with an accelerated radiation protocol. BMC Vet Res. 2017 Dec;13(1):86.
6. Ferrer-Jorda E, Rodríguez-Pizà I. Description of outcome and adverse events in 21 cats with locally advanced nasal planum squamous cell carcinoma treated with electrochemotherapy. J Feline Med Surg. 2024 July;26(7):1098612X241248043.
7. Gross TL, Ihrke PJ, Walder EJ, Affolter VK. Skin Diseases of the Dog and Cat: Clinical and Histopathologic Diagnosis. 2nd edn. Blackwell Publishing; 2005.
8. Simčič P, Pierini A, Lubas G, Lowe R, Granziera V, Tornago R, et al. A Retrospective Multicentric Study of Electrochemotherapy in the Treatment of Feline Nasal Planum Squamous Cell Carcinoma. Vet Sci. 2021 Mar 22;8(3):53.
9. Tellado M, Michinski S, Impellizeri J, Marshall G, Signori E, Maglietti F. Electrochemotherapy using thin-needle electrode improves recovery in feline nasal planum squamous cell carcinoma - a translational model. Cancer Drug Resist. 2022;5(3):595–611.
10. Lino M, Lanore D, Lajoinie M, Jimenez A, Crouzet F, Queiroga FL. Prognostic factors for cats with squamous cell carcinoma of the nasal planum following high-dose rate brachytherapy. J Feline Med Surg. 2019 Dec;21(12):1157–64.
11. Altamura G, Cardeti G, Cersini A, Eleni C, Cocumelli C, Bartolomé Del Pino LE, et al. Detection of *FELIS CATUS* papillomavirus type-2 DNA and viral gene expression suggest active infection in feline oral squamous cell carcinoma. Vet Comp Oncol. 2020 Dec;18(4):494–501.
12. Thomson M. Squamous Cell Carcinoma of the Nasal Planum in Cats and Dogs. Clin Tech Small Anim Pract. 2007 May;22(2):42–5.
13. Harris K, Gelberg HB, Kiupel M, Helfand SC. Immunohistochemical Features of Epithelial-Mesenchymal Transition in Feline Oral Squamous Cell Carcinoma. Vet Pathol. 2019 Nov;56(6):826–39.

14. Kummer S, Klang A, Strohmayr C, Walter I, Jindra C, Kneissl S, et al. Feline SCCs of the Head and Neck Display Partial Epithelial-Mesenchymal Transition and Harbor Stem Cell-like Cancer Cells. *Pathogens*. 2023 Oct 27;12(11):1288.
15. Armando F, Godizzi F, Razzuoli E, Leonardi F, Angelone M, Corradi A, et al. Epithelial to Mesenchymal Transition (EMT) in a Laryngeal Squamous Cell Carcinoma of a Horse: Future Perspectives. *Animals*. 2020 Dec 7;10(12):2318.
16. De Paolis L, Armando F, Montemurro V, Petrizzi L, Straticò P, Mecocci S, et al. Epithelial–mesenchymal transition in an EcPV2-positive vulvar squamous cell carcinoma of a mare. *Equine Vet J*. 2024 July;56(4):768–75.
17. Yamashita-Kawanishi N, Sawanobori R, Matsumiya K, Uema A, Chambers JK, Uchida K, et al. Detection of *felis catus* papillomavirus type 3 and 4 DNA from squamous cell carcinoma cases of cats in Japan. *J Vet Med Sci*. 2018;80(8):1236–40.
18. Munday JS. Papillomaviruses in felids. *Vet J*. 2014 Mar;199(3):340–7.
19. Munday JS, Gibson I, French AF. Papillomaviral DNA and increased p16CDKN2A protein are frequently present within feline cutaneous squamous cell carcinomas in ultraviolet-protected skin. *Vet Dermatol*. 2011 Aug;22(4):360–6.
20. Almeida EMP, Caraça RA, Adam RL, Souza EM, Metze K, Cintra ML. Photodamage in feline skin: clinical and histomorphometric analysis. *Vet Pathol*. 2008 May;45(3):327–35.
21. Brash DE. UV Signature Mutations. *Photochem Photobiol*. 2015 Jan;91(1):15–26.
22. Craene BD, Berx G. Regulatory networks defining EMT during cancer initiation and progression. *Nat Rev Cancer*. 2013 Feb;13(2):97–110.
23. Cowell RL, Valenciano AC. *Diagnostic Cytology and Hematology of the Dog and Cat*. 5th edn. Elsevier Mosby; 2020.
24. Stell AJ, Dobson JM, Langmack K. Photodynamic therapy of feline superficial squamous cell carcinoma using topical 5-aminolaevulinic acid. *J Small Anim Pract*. 2001 Apr;42(4):164–9.
25. Vail DM, Thamm DH, Liptak JM. *Withrow and MacEwen’s Small Animal Clinical Oncology*. 6th edn. Edra; 2020.
26. Millanta F, Parisi F, Poli A, Sorelli V, Abramo F. Auricular Non-Epithelial Tumors with Solar Elastosis in Cats: A Possible UV-Induced Pathogenesis. *Vet Sci*. 2022 Jan 18;9(2):34.
27. Scott D, Miller WH, Griffin CE. *Small Animal Dermatology*. 6th edn. Saunders; 2001.
28. Favrot C, Welle M, Heimann M, Godson DL, Guscelli F. Clinical, histologic, and immunohistochemical analyses of feline squamous cell carcinoma in situ. *Vet Pathol*. 2009 Jan;46(1):25–33.
29. Jarrett RH, Norman EJ, Gibson IR, Jarrett P. Curettage and diathermy: a treatment for feline nasal planum actinic dysplasia and superficial squamous cell carcinoma. *J Small Anim Pract*. 2013 Feb;54(2):92–8.

30. Munday JS, Kiupel M. Papillomavirus-Associated Cutaneous Neoplasia in Mammals. *Vet Pathol.* 2010 Mar;47(2):254–64.
31. Munday JS, Thomson NA, Luff JA. Papillomaviruses in dogs and cats. *Vet J.* 2017 July;225:23–31.
32. Bernard HU, Burk RD, Chen Z, van Doorslaer K, zur Hausen H, de Villiers EM. Classification of papillomaviruses (PVs) based on 189 PV types and proposal of taxonomic amendments. *Virology.* 2010 May 25;401(1):70–9.
33. Doorbar J, Quint W, Banks L, Bravo IG, Stoler M, Broker TR, et al. The biology and life-cycle of human papillomaviruses. *Vaccine.* 2012 Nov 20;30 Suppl 5:F55-70.
34. Hoggard N, Munday JS, Luff J. Localization of *Felis catus* Papillomavirus Type 2 E6 and E7 RNA in Feline Cutaneous Squamous Cell Carcinoma. *Vet Pathol.* 2018 May;55(3):409–16.
35. Munday JS, Knight CG, Luff JA. Papillomaviral skin diseases of humans, dogs, cats and horses: A comparative review. Part 1: Papillomavirus biology and hyperplastic lesions. *Vet J Lond Engl 1997.* 2022 Oct;288:105897.
36. Munday JS, Tucker RS, Kiupel M, Harvey CJ. Multiple oral carcinomas associated with a novel papillomavirus in a dog. *J Vet Diagn Investig Off Publ Am Assoc Vet Lab Diagn Inc.* 2015 Mar;27(2):221–5.
37. Zaugg N, Nespeca G, Hauser B, Ackermann M, Favrot C. Detection of novel papillomaviruses in canine mucosal, cutaneous and *in situ* squamous cell carcinomas. *Vet Dermatol.* 2005 Oct;16(5):290–8.
38. Sabattini S, Savini F, Gallina L, Scagliarini A, Bassi P, Bettini G. p16 Immunostaining of Canine Squamous Cell Carcinomas Is Not Associated with Papillomaviral DNA. *PLoS ONE.* 2016 July 21;11(7):e0159687.
39. Porcellato I, Brachelente C, Guelfi G, Reginato A, Sforza M, Bongiovanni L, et al. A retrospective investigation on canine papillomavirus 1 (CPV1) in oral oncogenesis reveals dogs are not a suitable animal model for high-risk HPV-induced oral cancer. *PloS One.* 2014;9(11):e112833.
40. Altamura G, Cuccaro B, Eleni C, Strohmayer C, Brandt S, Borzacchiello G. Investigation of multiple *Felis catus* papillomavirus types (-1/-2/-3/-4/-5/-6) DNAs in feline oral squamous cell carcinoma: a multicentric study. *J Vet Med Sci.* 2022 June 18;84(6):881–4.
41. Yamashita-Kawanishi N, Gushino Y, Chang CY, Chang HW, Chambers JK, Uchida K, et al. Full-genome characterization of a novel *Felis catus* papillomavirus 4 subtype identified in a cutaneous squamous cell carcinoma of a domestic cat. *Virus Genes.* 2021 Aug;57(4):380–4.
42. Carrai M, Van Brussel K, Shi M, Li CX, Chang WS, Munday JS, et al. Identification of a Novel Papillomavirus Associated with Squamous Cell Carcinoma in a Domestic Cat. *Viruses.* 2020 Jan 20;12(1):124.
43. Munday JS, Sharp CR, Beatty JA. Novel viruses: Update on the significance of papillomavirus infections in cats. *J Feline Med Surg.* 2019 May;21(5):409–18.

44. Altamura G, Power K, Martano M, Degli Uberti B, Galiero G, De Luca G, et al. Felis catus papillomavirus type-2 E6 binds to E6AP, promotes E6AP/p53 binding and enhances p53 proteasomal degradation. *Sci Rep*. 2018 Dec 3;8(1):17529.
45. Munday JS, French AF, Broughton L, Lin X, Bond SD, Kraberger S, et al. First Detection and Genetic Characterization of Felis catus Papillomavirus Type 11, the First Treisetapapillomavirus Type to Infect Domestic Cats. *Animals*. 2025 Jan;15(10):1416.
46. Chu S, Wylie TN, Wylie KM, Johnson GC, Skidmore ZL, Fleeer M, et al. A virome sequencing approach to feline oral squamous cell carcinoma to evaluate viral causative factors. *Vet Microbiol*. 2020 Jan;240:108491.
47. Altamura G, Corteggio A, Pacini L, Conte A, Pierantoni GM, Tommasino M, et al. Transforming properties of Felis catus papillomavirus type 2 E6 and E7 putative oncogenes in vitro and their transcriptional activity in feline squamous cell carcinoma in vivo. *Virology*. 2016 Sept;496:1–8.
48. Cruz-Gregorio A, Aranda-Rivera AK, Pedraza-Chaverri J. Pathological Similarities in the Development of Papillomavirus-Associated Cancer in Humans, Dogs, and Cats. *Anim Open Access J MDPI*. 2022 Sept 13;12(18):2390.
49. Altamura G, Borzacchiello G. Feline oral squamous cell carcinoma and Felis catus papillomavirus: is it time to walk the path of human oncology? *Front Vet Sci*. 2023 May 17;10:1148673.
50. Moody CA, Laimins LA. Human papillomavirus oncoproteins: pathways to transformation. *Nat Rev Cancer*. 2010 Aug;10(8):550–60.
51. Doorbar J. The papillomavirus life cycle. *J Clin Virol Off Publ Pan Am Soc Clin Virol*. 2005 Mar;32 Suppl 1:S7-15.
52. De Morais EF, Rolim LSA, De Melo Fernandes Almeida DR, De Farias Morais HG, De Souza LB, De Almeida Freitas R. Biological role of epithelial–mesenchymal-transition-inducing transcription factors in head and neck squamous cell carcinoma: A systematic review. *Arch Oral Biol*. 2020 Nov;119:104904.
53. Nishida A, Andoh A. The Role of Inflammation in Cancer: Mechanisms of Tumor Initiation, Progression, and Metastasis. *Cells*. 2025 Mar 25;14(7):488.
54. Parisi F, Fonti N, Millanta F, Freer G, Pistello M, Poli A. Exploring the link between viruses and cancer in companion animals: a comprehensive and comparative analysis. *Infect Agent Cancer*. 2023 June 29;18(1):40.
55. Armando F, Mecocci S, Orlandi V, Porcellato I, Cappelli K, Mechelli L, et al. Investigation of the Epithelial to Mesenchymal Transition (EMT) Process in Equine Papillomavirus-2 (EcPV-2)-Positive Penile Squamous Cell Carcinomas. *Int J Mol Sci*. 2021 Sept 30;22(19):10588.
56. Armando F, Porcellato I, De Paolis L, Mecocci S, Passeri B, Ciurkiewicz M, et al. Vulvo-vaginal epithelial tumors in mares: A preliminary investigation on epithelial-mesenchymal transition and tumor-immune microenvironment. *Vet Pathol*. 2024 May;61(3):366–81.

57. Munday JS, Bell CM, Gulliver EL. Feline oral in situ carcinoma associated with papillomavirus infection: A case series of 7 cats. *Vet Pathol.* 2025 July 3;3009858251352594.
58. Lewis JS. p16 Immunohistochemistry As a Standalone Test for Risk Stratification in Oropharyngeal Squamous Cell Carcinoma. *Head Neck Pathol.* 2012 July;6(S1):75–82.
59. Sano T, Oyama T, Kashiwabara K, Fukuda T, Nakajima T. Expression Status of p16 Protein Is Associated with Human Papillomavirus Oncogenic Potential in Cervical and Genital Lesions. *Am J Pathol.* 1998 Dec;153(6):1741–8.
60. Ang KK, Harris J, Wheeler R, Weber R, Rosenthal DI, Nguyen-Tân PF, et al. Human Papillomavirus and Survival of Patients with Oropharyngeal Cancer. *N Engl J Med.* 2010 July;363(1):24–35.
61. Kalluri R, Weinberg RA. The basics of epithelial-mesenchymal transition. *J Clin Invest.* 2009 June 1;119(6):1420–8.
62. Lamouille S, Xu J, Derynck R. Molecular mechanisms of epithelial–mesenchymal transition. *Nat Rev Mol Cell Biol.* 2014 Mar;15(3):178–96.
63. Thiery JP, Acloque H, Huang RYJ, Nieto MA. Epithelial-mesenchymal transitions in development and disease. *Cell.* 2009 Nov 25;139(5):871–90.
64. Lim J, Thiery JP. Epithelial-mesenchymal transitions: insights from development. *Dev Camb Engl.* 2012 Oct;139(19):3471–86.
65. Nieto MA, Huang RYJ, Jackson RA, Thiery JP. EMT: 2016. *Cell.* 2016 June;166(1):21–45.
66. Acloque H, Adams MS, Fishwick K, Bronner-Fraser M, Nieto MA. Epithelial-mesenchymal transitions: the importance of changing cell state in development and disease. *J Clin Invest.* 2009 June;119(6):1438–49.
67. Sauka-Spengler T, Bronner-Fraser M. A gene regulatory network orchestrates neural crest formation. *Nat Rev Mol Cell Biol.* 2008 July;9(7):557–68.
68. Person AD, Klewer SE, Runyan RB. Cell biology of cardiac cushion development. *Int Rev Cytol.* 2005;243:287–335.
69. Nawshad A, Medici D, Liu CC, Hay ED. TGFbeta3 inhibits E-cadherin gene expression in palate medial-edge epithelial cells through a Smad2-Smad4-LEF1 transcription complex. *J Cell Sci.* 2007 May 1;120(Pt 9):1646–53.
70. Pastushenko I, Blanpain C. EMT Transition States during Tumor Progression and Metastasis. *Trends Cell Biol.* 2019 Mar;29(3):212–26.
71. Zeisberg M, Neilson EG. Biomarkers for epithelial-mesenchymal transitions. *J Clin Invest.* 2009 June;119(6):1429–37.
72. Lovisa S, LeBleu VS, Tampe B, Sugimoto H, Vадnagara K, Carstens JL, et al. Epithelial-to-mesenchymal transition induces cell cycle arrest and parenchymal damage in renal fibrosis. *Nat Med.* 2015 Sept;21(9):998–1009.

73. Grande MT, López-Novoa JM. Fibroblast activation and myofibroblast generation in obstructive nephropathy. *Nat Rev Nephrol.* 2009 June;5(6):319–28.
74. Willis BC, Liebler JM, Luby-Phelps K, Nicholson AG, Crandall ED, du Bois RM, et al. Induction of Epithelial-Mesenchymal Transition in Alveolar Epithelial Cells by Transforming Growth Factor- β 1. *Am J Pathol.* 2005 May;166(5):1321–32.
75. Choi SS, Diehl AM. Epithelial-to-mesenchymal transitions in the liver. *Hepatology* Baltim Md. 2009 Dec;50(6):2007–13.
76. Dominguez C, David JM, Palena C. Epithelial-mesenchymal transition and inflammation at the site of the primary tumor. *Semin Cancer Biol.* 2017 Dec;47:177–84.
77. Chaffer CL, Weinberg RA. A perspective on cancer cell metastasis. *Science.* 2011 Mar 25;331(6024):1559–64.
78. Grivennikov SI, Greten FR, Karin M. Immunity, inflammation, and cancer. *Cell.* 2010 Mar 19;140(6):883–99.
79. Dongre A, Weinberg RA. New insights into the mechanisms of epithelial-mesenchymal transition and implications for cancer. *Nat Rev Mol Cell Biol.* 2019 Feb;20(2):69–84.
80. Terry S, Savagner P, Ortiz-Cuaran S, Mahjoubi L, Saintigny P, Thiery JP, et al. New insights into the role of EMT in tumor immune escape. *Mol Oncol.* 2017 July;11(7):824–46.
81. Singh A, Settleman J. EMT, cancer stem cells and drug resistance: an emerging axis of evil in the war on cancer. *Oncogene.* 2010 Aug 26;29(34):4741–51.
82. Brabletz T, Kalluri R, Nieto MA, Weinberg RA. EMT in cancer. *Nat Rev Cancer.* 2018 Feb;18(2):128–34.
83. Vesuna F, Lisok A, Kimble B, Raman V. Twist modulates breast cancer stem cells by transcriptional regulation of CD24 expression. *Neoplasia* N Y N. 2009 Dec;11(12):1318–28.
84. Peinado H, Olmeda D, Cano A. Snail, Zeb and bHLH factors in tumour progression: an alliance against the epithelial phenotype? *Nat Rev Cancer.* 2007 June;7(6):415–28.
85. Morel AP, Lièvre M, Thomas C, Hinkal G, Ansieau S, Puisieux A. Generation of breast cancer stem cells through epithelial-mesenchymal transition. *PloS One.* 2008 Aug 6;3(8):e2888.
86. Scheel C, Weinberg RA. Cancer stem cells and epithelial-mesenchymal transition: concepts and molecular links. *Semin Cancer Biol.* 2012 Oct;22(5–6):396–403.
87. Zhang W, Wu X, Hu L, Ma Y, Xiu Z, Huang B, et al. Overexpression of Human Papillomavirus Type 16 Oncoproteins Enhances Epithelial–Mesenchymal Transition via STAT3 Signaling Pathway in Non-Small Cell Lung Cancer Cells. *Oncol Res.* 2017 May 24;25(5):843–52.
88. Ashrafizadeh M, Zarrabi A, Hushmandi K, Kalantari M, Mohammadinejad R, Javaheri T, et al. Association of the Epithelial-Mesenchymal Transition (EMT) with Cisplatin Resistance. *Int J Mol Sci.* 2020 June 3;21(11):4002.

89. Luo Y, Yu T, Zhang Q, Fu Q, Hu Y, Xiang M, et al. Upregulated N-cadherin expression is associated with poor prognosis in epithelial-derived solid tumours: A meta-analysis. *Eur J Clin Invest*. 2018 Apr;48(4):e12903.
90. Ghittoni R, Accardi R, Chiocca S, Tommasino M. Role of human papillomaviruses in carcinogenesis. *Ecancermedicalsecience*. 2015;9:526.
91. Wheelock MJ, Shintani Y, Maeda M, Fukumoto Y, Johnson KR. Cadherin switching. *J Cell Sci*. 2008 Mar 15;121(Pt 6):727–35.
92. Berx G, van Roy F. Involvement of Members of the Cadherin Superfamily in Cancer. *Cold Spring Harb Perspect Biol*. 2009 Dec;1(6):a003129.
93. Cavallaro U, Christofori G. Cell adhesion and signalling by cadherins and Ig-CAMs in cancer. *Nat Rev Cancer*. 2004 Feb;4(2):118–32.
94. Satelli A, Li S. Vimentin in cancer and its potential as a molecular target for cancer therapy. *Cell Mol Life Sci CMLS*. 2011 Sept;68(18):3033–46.
95. Heuberger J, Birchmeier W. Interplay of cadherin-mediated cell adhesion and canonical Wnt signaling. *Cold Spring Harb Perspect Biol*. 2010 Feb;2(2):a002915.
96. Yang S wei, Zhang Z gang, Hao Y xue, Zhao Y liang, Qian F, Shi Y, et al. HIF-1 α induces the epithelial-mesenchymal transition in gastric cancer stem cells through the Snail pathway. *Oncotarget*. 2017 Jan 4;8(6):9535–45.
97. Chaffer CL, Marjanovic ND, Lee T, Bell G, Kleer CG, Reinhardt F, et al. Poised chromatin at the ZEB1 promoter enables breast cancer cell plasticity and enhances tumorigenicity. *Cell*. 2013 July 3;154(1):61–74.
98. Semenza GL. Hypoxia-inducible factor 1: master regulator of O₂ homeostasis. *Curr Opin Genet Dev*. 1998 Oct 1;8(5):588–94.
99. Zhang W, Shi X, Peng Y, Wu M, Zhang P, Xie R, et al. HIF-1 α Promotes Epithelial-Mesenchymal Transition and Metastasis through Direct Regulation of ZEB1 in Colorectal Cancer. *PloS One*. 2015;10(6):e0129603.
100. Ghittoni R, Accardi R, Hasan U, Gheit T, Sylla B, Tommasino M. The biological properties of E6 and E7 oncoproteins from human papillomaviruses. *Virus Genes*. 2010 Feb;40(1):1–13.
101. Wang H, Liu C, Jin K, Li X, Zheng J, Wang D. Research advances in signaling pathways related to the malignant progression of HSIL to invasive cervical cancer: A review. *Biomed Pharmacother*. 2024 Nov 1;180:117483.
102. Altamura G, Corteggio A, Borzacchiello G. *Felis catus* papillomavirus type 2 E6 oncogene enhances mitogen-activated protein kinases and Akt activation but not EGFR expression in an in vitro feline model of viral pathogenesis. *Vet Microbiol*. 2016 Nov 15;195:96–100.
103. Kowli S, Velidandla R, Creek KE, Pirisi L. TGF- β Regulation of Gene Expression at Early and Late Stages of HPV16-Mediated Transformation of Human Keratinocytes. *Virology*. 2013 Dec;447(0):63–73.

104. Trugilo KP, Cebinelli GCM, Castilha EP, da Silva MR, Berti FCB, de Oliveira KB. The role of transforming growth factor β in cervical carcinogenesis. *Cytokine Growth Factor Rev.* 2024 Dec;80:12–23.
105. González-González R, Ortiz-Sarabia G, Molina-Frechero N, Salas-Pacheco JM, Salas-Pacheco SM, Lavallo-Carrasco J, et al. Epithelial–Mesenchymal Transition Associated with Head and Neck Squamous Cell Carcinomas: A Review. *Cancers.* 2021 June 17;13(12):3027.
106. Hatakeyama H, Mizumachi T, Kano S, Homma A, Fukuda S. Epithelial-Mesenchymal Transition in HPV-Positive and-Negative Oropharyngeal Squamous Cell Carcinoma. *Otolaryngol Neck Surg [Internet].* 2013 Sept [cited 2025 June 23];149(S2). Available from: <https://aao-hnsfjournals.onlinelibrary.wiley.com/doi/10.1177/0194599813495815a89>
107. Noubissi Nzeteu GA, Geismann C, Arlt A, Hoogwater FJH, Nijkamp MW, Meyer NH, et al. Role of Epithelial-to-Mesenchymal Transition for the Generation of Circulating Tumors Cells and Cancer Cell Dissemination. *Cancers.* 2022 Nov 8;14(22):5483.
108. Allgayer H, Mahapatra S, Mishra B, Swain B, Saha S, Khanra S, et al. Epithelial-to-mesenchymal transition (EMT) and cancer metastasis: the status quo of methods and experimental models 2025. *Mol Cancer.* 2025 June 7;24:167.
109. Onder TT, Gupta PB, Mani SA, Yang J, Lander ES, Weinberg RA. Loss of E-cadherin promotes metastasis via multiple downstream transcriptional pathways. *Cancer Res.* 2008 May 15;68(10):3645–54.
110. Ren X, Wang J, Lin X, Wang X. E-cadherin expression and prognosis of head and neck squamous cell carcinoma: evidence from 19 published investigations. *OncoTargets Ther.* 2016 Apr 26;9:2447–53.
111. Puneeta N, Santosh T, Mishra I, Gaikwad P, Sahu A. Evaluation of e-cadherin and vimentin expression for different grades of oral epithelial dysplasia and oral squamous cell carcinoma - An immunohistochemical study. *J Oral Maxillofac Pathol JOMFP.* 2022;26(2):285–6.
112. Fontan CT, Das D, Bristol ML, James CD, Wang X, Lohner H, et al. Human Papillomavirus 16 (HPV16) E2 Repression of TWIST1 Transcription Is a Potential Mediator of HPV16 Cancer Outcomes. *mSphere.* 2020 Dec 9;5(6):e00981-20.
113. Munday JS, Knight CG, Bodaan CJ, Codaccioni C, Hardcastle MR. Equus caballus papillomavirus Type 7 is a rare cause of equine penile squamous cell carcinomas. *Vet J Lond Engl 1997.* 2024 Aug;306:106155.
114. Casas E, Kim J, Bendesky A, Ohno-Machado L, Wolfe CJ, Yang J. Snail2 is an essential mediator of Twist1-induced epithelial mesenchymal transition and metastasis. *Cancer Res.* 2011 Jan 1;71(1):245–54.
115. Yang J, Mani SA, Donaher JL, Ramaswamy S, Itzykson RA, Come C, et al. Twist, a master regulator of morphogenesis, plays an essential role in tumor metastasis. *Cell.* 2004 June 25;117(7):927–39.

116. Wangmo C, Charoen N, Jantharapattana K, Dechaphunkul A, Thongsuksai P. Epithelial–Mesenchymal Transition Predicts Survival in Oral Squamous Cell Carcinoma. *Pathol Oncol Res.* 2020 July;26(3):1511–8.
117. Munday JS, Knight CG, Luff JA. Papillomaviral skin diseases of humans, dogs, cats and horses: A comparative review. Part 2: Pre-neoplastic and neoplastic diseases. *Vet J Lond Engl* 1997. 2022 Oct;288:105898.
118. Tutu P, Daraban Bocaneti F, Altamura G, Dascalu MA, Horodincu L, Soreanu OD, et al. Feline oral squamous cell carcinoma: recent advances and future perspectives. *Front Vet Sci.* 2025;12:1663990.
119. Ito S, Chambers JK, Sumi A, Yamashita-Kawanishi N, Omachi T, Haga T, et al. Involvement of *Felis catus* papillomavirus type 2 in the tumorigenesis of feline Merkel cell carcinoma. *Vet Pathol.* 2022 Jan;59(1):63–74.
120. Barillari G, Bei R, Manzari V, Modesti A. Infection by High-Risk Human Papillomaviruses, Epithelial-to-Mesenchymal Transition and Squamous Pre-Malignant or Malignant Lesions of the Uterine Cervix: A Series of Chained Events? *Int J Mol Sci.* 2021 Dec 17;22(24):13543.
121. Altamura G, Borzacchiello G. HPV related head and neck squamous cell carcinoma: New evidences for an emerging spontaneous animal model. *Oral Oncol.* 2019 Jan;88:84.
122. the Papillophar Study Group, Lefevre M, Rousseau A, Rayon T, Dalstein V, Clavel C, et al. Epithelial to mesenchymal transition and HPV infection in squamous cell oropharyngeal carcinomas: the papillophar study. *Br J Cancer.* 2017 Jan;116(3):362–9.
123. Strohmayer C, Klang A, Kummer S, Walter I, Jindra C, Weissenbacher-Lang C, et al. Tumor Cell Plasticity in Equine Papillomavirus-Positive Versus-Negative Squamous Cell Carcinoma of the Head and Neck. *Pathogens.* 2022 Feb 18;11(2):266.
124. Bedard MC, Rivera-Cruz CM, Chihanga T, VonHandorf A, Tang AL, Zender C, et al. A Single-Cell Transcriptome Atlas of Epithelial Subpopulations in HPV-Positive and HPV-Negative Head and Neck Cancers. *Viruses.* 2025 Mar 24;17(4):461.
125. Ida S, Takahashi H, Tada H, Mito I, Matsuyama T, Chikamatsu K. Dynamic changes of the EMT spectrum between circulating tumor cells and the tumor microenvironment in human papillomavirus-positive head and neck squamous cell carcinoma. *Oral Oncol.* 2023 Feb;137:106296.